Gold mineralization in the St Ives camp near Kambalda

by

P. Neumayr[1], J. Walshe[2], K. Connors[3], S. Cox[4], R. S. Morrison[3], and E. Stolz[3]

Introduction

This contribution describes the geological and structural settings, and structural controls on gold mineralization, as well as camp- to deposit-scale hydrothermal alteration footprints in the St Ives gold camp (Fig. 1). The aim of the visit to St Ives is to show:

- the structural architecture of the camp;
- the structural and stratigraphic setting of gold deposits,
- typical mineralization styles;
- different alteration styles and alteration footprints in the camp.

Subject to mine schedules, the excursion will visit the Argo and Greater Revenge deposits, and excursion participants will have the opportunity to examine representative diamond drillcore showing mineralization and alteration styles.

Discovery and mining history

The St Ives gold camp is located about 55 km south-southeast of Kalgoorlie (Fig. 1). St Ives Gold Mining Company, a wholly owned subsidiary of Gold Fields Ltd, is currently the second-largest gold-mining operation in Australia, producing about 500 000 ounces of gold per annum.

Gold was discovered at Kambalda (the ‘Red Hill Camp’) in 1897 and, between 1897 and 1907, the gold workings of the area supported a small township. Other gold-bearing locations, such as Victory, were discovered at this time. A total gold production of 31 000 ozs is recorded for this period, mostly from the Red Hill group of mines. Thereafter, the area attracted only intermittent attention of prospectors until 1919, when a significant new discovery was made at St Ives. Another small town was constructed, but soon abandoned when the mine closed in about 1926.

Gold prospecting activity continued until Fe–Ni sulfides were discovered in 1966 near the old Red Hill mine. Gossanous outcrop collected by uranium prospectors in 1954 was brought to the attention of Western Mining Corporation (WMC) in 1964. The ground was acquired by WMC, and geological mapping, and geochemical and geophysical surveys were completed in the area of the Kambalda Dome. Several anomalies and gossans were identified at the basal contact of the ultramafic unit. Drilling (diamond drillhole KD-1) of the gossan near Red Hill commenced at the end of 1965, and resulted in the discovery of the Lunnon shoot in January 1966. This orebody, and others discovered shortly thereafter, formed the resource base of Kambalda Nickel Operation (KNO). A mining and milling operation was developed rapidly, and transport of nickel concentrates from Kambalda commenced in mid-1967. Production increased rapidly and exceeded 30 000 t of nickel metal in 1970–71. This production represented about 8% of the western world production. WMC constructed a refinery at Kwinana in 1970, and a smelter at Kalgoorlie in 1972. A major new industry had been established. Total historical production for the greater Kambalda nickel mining district from 1967 to 1996 is about 34 Mt at 3.1% nickel, for more than 1 Mt of nickel metal in concentrate.

An increase in the price of gold in the late 1970s provided the impetus for re-evaluation of the old gold prospects in the Kambalda area. It was soon recognized that significant gold mineralization remained, particularly in the Victory area, and exploration effort substantially increased in the early 1980s. Gold production recommenced in 1981 and has since expanded with the construction of a 3 Mt per annum mill at St Ives. Annual gold production reached 400 000 ozs in 1996. From commissioning until May 1998, the plant processed almost 27 Mt of ore to produce just over 3 million ounces (Moz) of gold.

[1] pdm*CRC; Centre for Global Metallogeny, The University of Western Australia, 35 Stirling Highway, Crawley, W.A. 6009, Australia

[2] pmd*CRC; Division for Exploration and Mining, CSIRO, 26 Dick Perry Avenue, Kensington, W.A. 6151, Australia

[3] St Ives Gold Mining Company Pty Ltd, Post Office, Kambalda, W.A. 6444, Australia

[4] Research School of Earth Sciences and Department of Geology, The Australian National University, Canberra, A.C.T. 2600, Australia

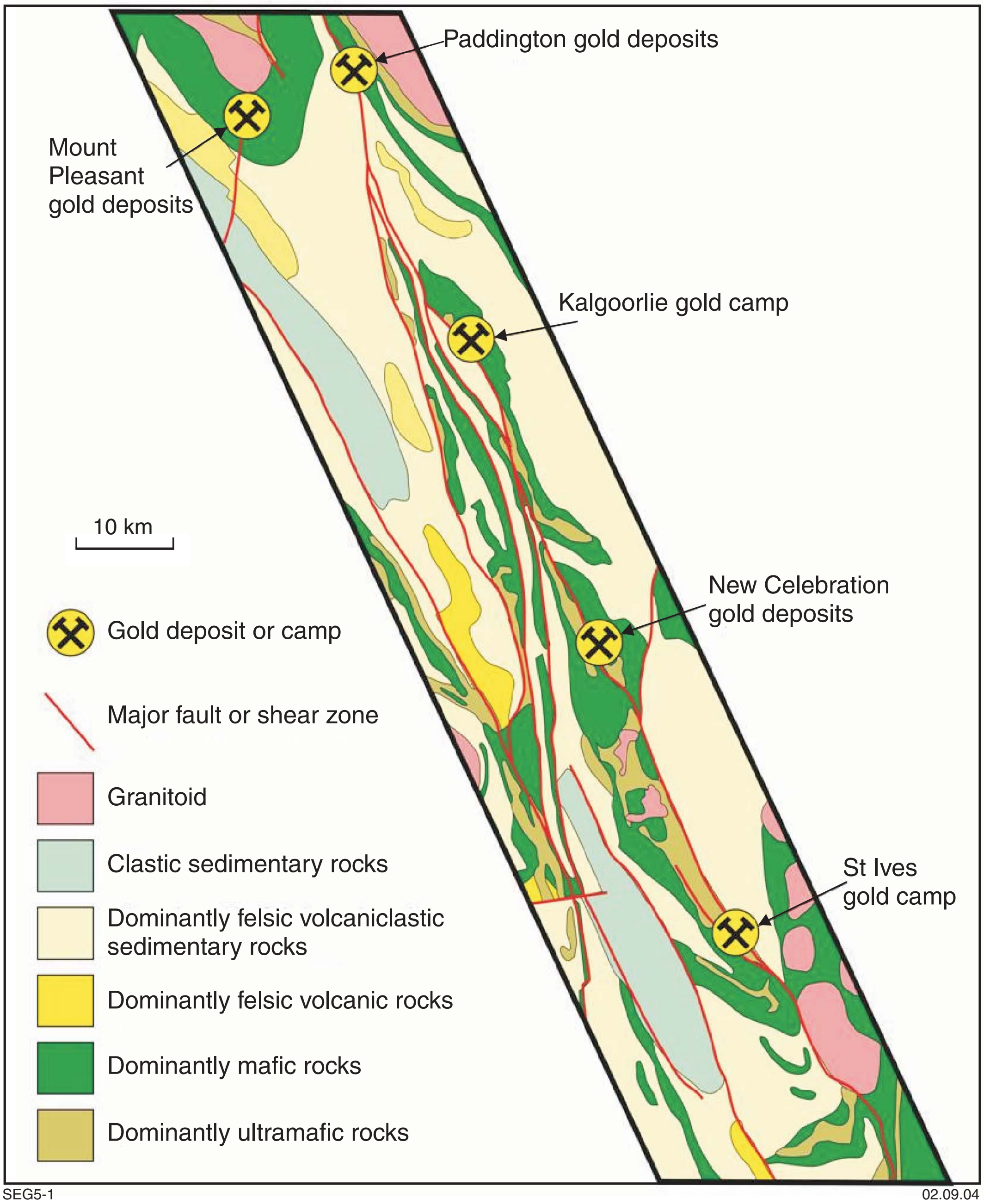

Figure 1. Location of the St Ives gold camp

Since Gold Fields purchased the properties for US$232 million in 2001, the camp has seen an unprecedented exploration effort, mainly in the Greater Revenge, Argo, and Intrepide complexes, and a total of A$30 million was spent on reserve replacement and reserve expansion work in the 2003 financial year. In late 2003, Gold Fields announced plans to construct a new A$125 million, 4.5 Mtpa gold-processing facility at St Ives. At present, St Ives Gold Mining Company operates three underground mines (Junction, Argo, and Leviathan) and two openpit complexes (Greater Revenge and Argo). In the 2003 financial year, 513 000 oz of gold were produced from the camp.

Geological setting of the St Ives gold camp

Introduction

The St Ives gold camp is located in the Archaean Norseman–Wiluna greenstone belt of the Yilgarn Craton of Western Australia (Figs 1 and 2). The Norseman–Wiluna greenstone belt (Gee, 1979; Gee et al., 1981) is a north-northwesterly trending belt that extends about 200 km in width and 800 km in strike length, and is part of the Eastern Goldfields Province (McNaughton and

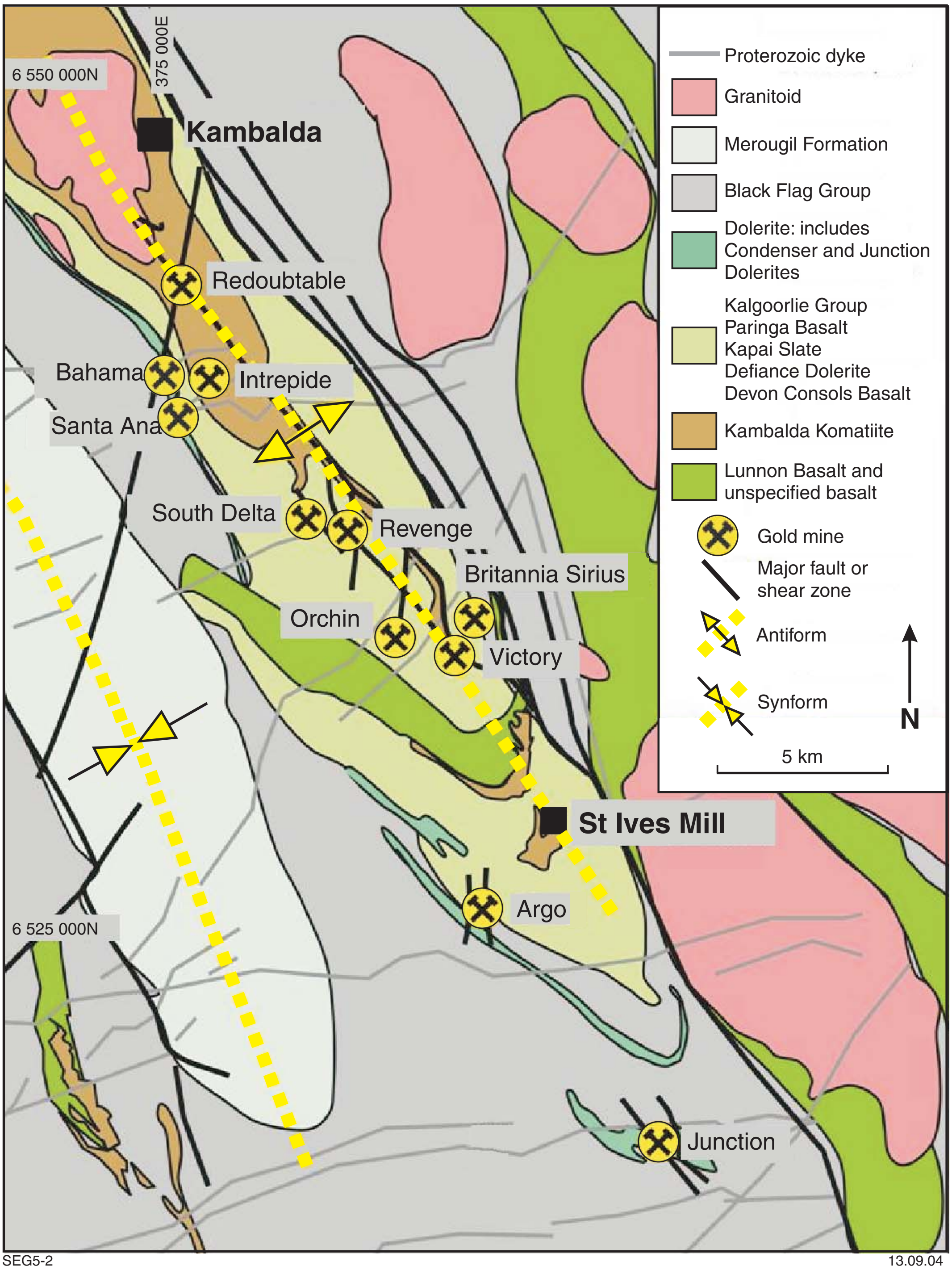

Figure 2. Geology and location of gold deposits in the St Ives gold camp

Dahl, 1987). It comprises successions of tholeiitic and komatiitic volcanic rocks, felsic–intermediate intrusive rocks, and volcanoclastic and epiclastic sedimentary rocks (Gee, 1979; Gee et al., 1981). The belt is intruded by numerous granitoids and porphyry swarms, and is characterized by the absence of banded iron-formation (BIF) marker horizons. The Norseman–Wiluna greenstone belt hosts over two-thirds of Australia's known Archaean gold endowment (Woodall, 1990).

Stratigraphy

Stratigraphic sequence

In the Kambalda – St Ives area, the Norseman–Wiluna greenstone belt consists mainly of mafic–ultramafic lavas and intrusions (Figs 2, 3, and 4; Table 1), and is bound by the Lefroy Fault to the east and the Merougil Fault to the west (Nguyen et al., 1998). In the following descriptions,

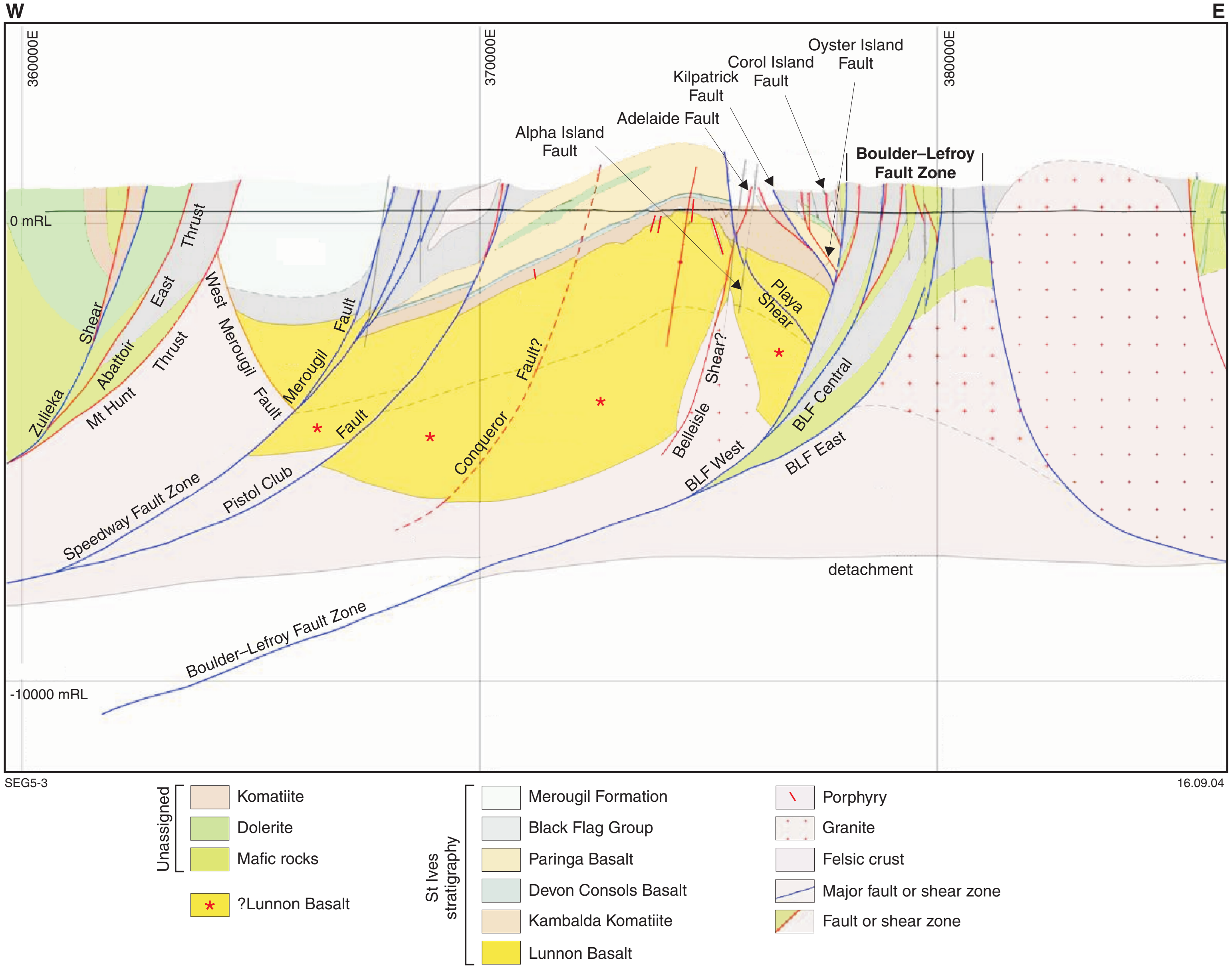

Figure 3. Cross section at 6545020N in the Intrepide area showing geological and structural setting of the St Ives gold camp

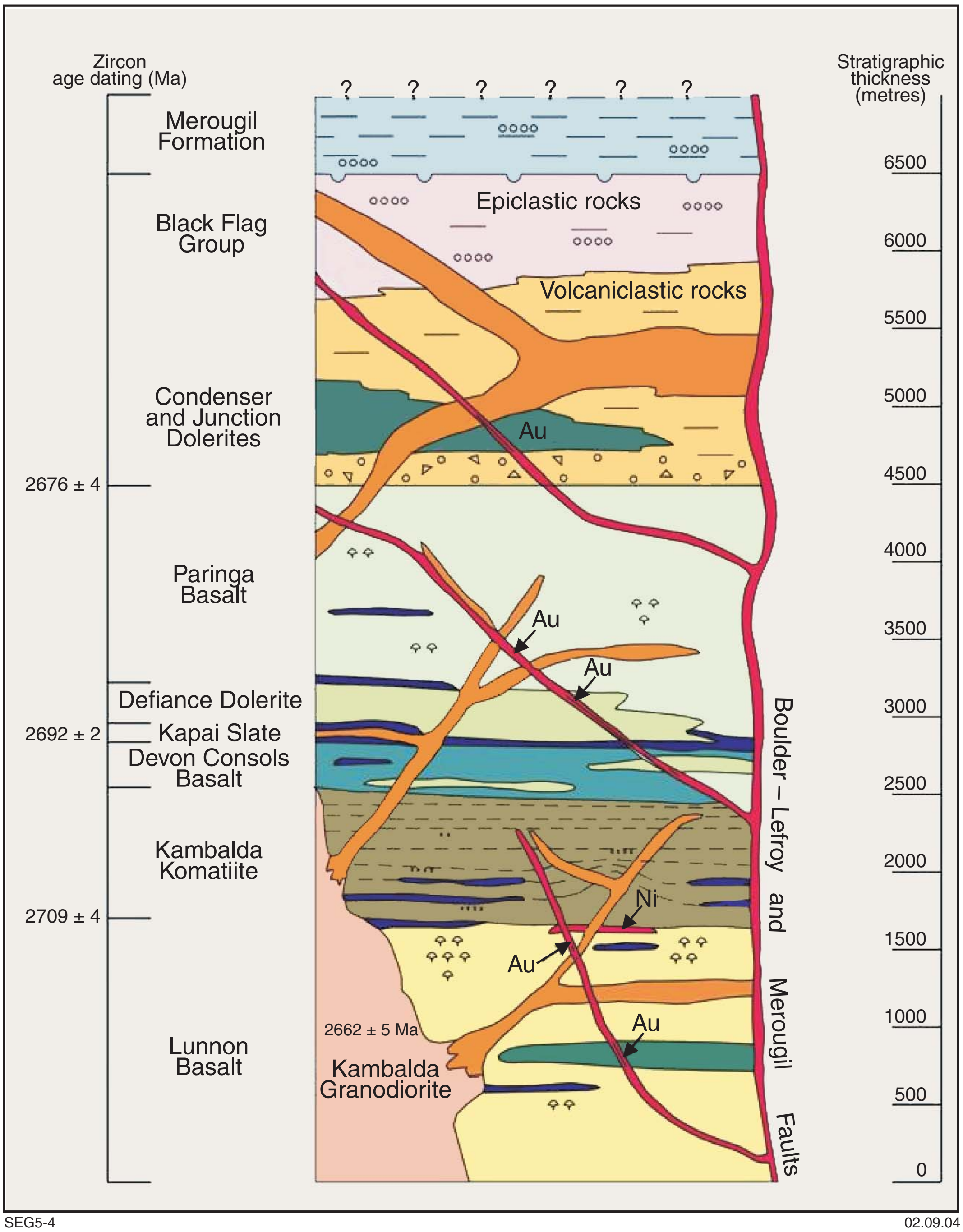

Figure 4. Stratigraphic relationships in the St Ives gold camp, based on the Kambalda–Tramways stratigraphy (after Cowden and Archibald, 1987)

Table 1. Summary of main stratigraphic units in the Kambalda–Kalgoorlie region

Group	Formation	Age (Ma)	Notes
	Merougil Formation	2664 ± 6	Hand (1996)
Black Flag Group	Morgans Island Epiclastic Formation	2666–2669	Hand (1996); locality just south of Kalgoorlie but most Black Flag Group must predate D_1 deformation at c. 2675 Ma, consistent with the 2676 ± 4 Ma age of a crystal tuff unit from the Kambalda area (quoted in Connors et al., 2003)
	Newton Felsic Formation		
Kalgoorlie Group	Paringa Basalt	2690 ± 5	Quoted in Connors et al. (2003)
	Kapai Slate	2692 ± 4	Claoué-Long et al. (1988)
	Devon Consols Basalt	2693 ± 30	Compston et al. (1986)
	Kambalda Komatiite	2709 ± 4	Quoted in Connors et al. (2003)
	Lunnon Basalt	2726± 30	Chauvel et al. (1985)

all Archaean rocks are metamorphosed, and the prefix 'meta' is omitted but implied.

Kalgoorlie Group

Lunnon Basalt

The Lunnon Basalt is the lowest stratigraphic formation in the Kalgoorlie Group. It is a thick (>2000 m, and up to 5 km based on three-dimensional gravity models) tholeiitic basalt sequence that consists of thin (2–3 m) lava flows, minor interflow sedimentary rocks, and concordant dolerite dykes (Watchorn, 1998). Pillowed zones are common in the basalt, but vesicles (varioles) are rare. The basalt is a low-magnesium pillow basalt, with MgO content ranging from 6 to 7% at the Foster Thrust (Nguyen, 1997). The formation is conformably overlain by the Silver Lake Member of the Kambalda Komatiite.

Kambalda Komatiite

The Kambalda Komatiite is a 100 to >1200 m-thick sequence of high-MgO ultramafic flows (Watchorn, 1998). The sequence has been subdivided into the lower Silver Lake Member and the upper Tripod Hill Member (Gresham and Loftus-Hill, 1981). The volcaniclastic sedimentary unit near the base of the komatiite has been dated at 2709 ± 4 Ma (Claoué-Long et al., 1988). The massive-sulfide nickel orebodies of the Kambalda area occur at the basal contact of the Silver Lake Member with the Lunnon Basalt. The Silver Lake Member consists of one or more, 10–100 m-thick, komatiite flows, which are subdivided into a lower cumulate zone, with up to 48% MgO, and an upper spinifex-textured zone. Numerous lenticular interflow sedimentary rocks are interleaved with the komatiite lavas. The Tripod Hill Member consists of thin (<0.5 to 10 m) komatiite lava flows, which reach a combined thickness of up to 700 m. The upper komatiite flows are more differentiated than those of the Silver Lake Member, and contain less abundant interflow sedimentary rocks.

Devon Consols Basalt

The contact of the Devon Consols Basalt with the underlying Tripod Hill Komatiite is typically gradational (interfingering) but locally sharp (Gresham and Loftus-Hill, 1981; Cowden and Roberts, 1990). The unit, previously documented as being 60–100 m thick, has been noted at over 150 m thick in the Greater Revenge area. It is composed of pillowed and massive variolitic lava flows and thin differentiated synvolcanic dolerites (Victory and Trafalgar Dolerites). The Victory Dolerite is internally zoned, with an ultramafic pyroxenite base to ophitic gabbro, but granophyre is absent and there is no evidence for systematic Fe-enrichment (MacGeehan, 1984).

The Devon Consols Basalt pillowed sections are distinctively variolitic. Field exposures typically have a nodular, warty appearance due to differential weathering of the varioles. The varioles are up to 2 cm in diameter, felsic (white to pale yellowish-green), and are concentrated in the central zones of pillows. Aphyric hyaloclastite fragments occupy interpillow spaces. The differentiated units comprise fine-grained basaltic upper zones and coarse-grained gabbroic lower zones. The major metamorphic mineral assemblage of the Devon Consols Basalt is actinolite–chlorite–zoisite–albite, with about 30% actinolite.

Geochemically, the Devon Consols Basalt has been divided into two types (Redman and Keays, 1985): (1) high-Si, low-Mg basalts (52–60% SiO_2, 4–6% MgO); and (2) low-Si, high-Mg basalts (47–52% SiO_2, 9–16% MgO). The two geochemical types have Al_2O_3/TiO_2 ratios of about 20 and are enriched in LREE ($[La/Sm]_n$ ratio = 1.2–1.3). The Nd isotopic data of ε_{Nd} range from +1.2 to -3 (Foster, 1993), and indicate melt derivation from a long-term depleted source (Lesher and Arndt, 1995). These rocks are considered by Lesher and Arndt (1995) to be komatiitic basalts formed from crustally contaminated komatiitic melt. This interpretation is consistent with the presence of xenocrystic zircons older than 3400–3100 Ma in the Victory Dolerite (Compston et al., 1986; Claoué-

Long et al., 1988). The morphology of the zircons suggests derivation from felsic granulite (Compston et al., 1986). All the data suggest that the Devon Consols Basalt parental melts interacted with very old felsic granulite basement, or eroded products thereof, and were contaminated by up to 5–7% continental crust (Lesher and Arndt, 1995).

Kapai Slate

The Kapai Slate marks the boundary between the underlying Devon Consols Basalt and the overlying Paringa Basalt, and occurs throughout the Kambalda Dome – St Ives – Tramways area. The Kapai Slate is up to 10 m thick, but is typically intruded by intermediate to felsic sills.

Siliceous sedimentary facies of the Kapai Slate are considered to represent a combination of tuffaceous debris from distal felsic volcanic eruptions, and minor chemical deposition from silica-rich exhalations. In an alternative interpretation, these zones have been silicified after their deposition. The interpretation of a tuffaceous component is consistent with the presence of 2692 ± 4 Ma magmatic zircons in these rocks (Claoué-Long et al., 1988). Rare xenocrystic zircons as old as 3450 Ma have been identified, and could indicate pre-existing continental crust (Claoué-Long et al., 1988). Carbonaceous facies of the Kapai Slate probably originated from non-photosynthetic bacteria and cyanobacteria inhabiting quiescent sea-floor environments. A sulfide-rich facies is interpreted by Marsh (1988) to have been deposited in an active extensional basin where sea-floor hydrothermal alteration was intense.

Paringa Basalt

The Paringa Basalt is 500–1500 m thick, and consists of thin variolitic, pillowed flows and thick, differentiated dolerite units, such as the Defiance Dolerite (Carey, 1994).

Basalt facies

Pillows display 2–3 cm-thick rinds and chlorite-rich varioles. The varioles are markedly less prominent than in the Devon Consols Basalt (see above). Interpillow breccias are common and broad zones of hyaloclastite breccia are developed close to the base. Thin, laminated interflow cherty sedimentary units are present close to the base of the unit (Balkau, 1989).

The metamorphic assemblage of the Paringa Basalt is actinolite–chlorite–biotite–albite–epidote–clinozoisite–quartz and Fe–Ti oxides. Where igneous textures are preserved, the basalts appear to have been clinopyroxene-phyric. Clinopyroxene is replaced by biotite, chlorite and actinolite.

Geochemically, the Paringa Basalt has high magnesium (12–16% MgO) and silica (49–57% SiO_2) contents (Redman and Keays, 1985). The Al_2O_3/TiO_2 ratios average about 20. Thicker differentiated flows or sills contain coarse-grained gabbroic (6–8% MgO) upper parts and ultramafic (22–24% MgO) lower parts. The Paringa Basalt has $[La/Sm]_n$ ratios of 2.5–2.8 and negative ε_{Nd} values, which together have been interpreted to indicate up to 25% crustal contamination (Lesher and Arndt, 1995). Sensitive high resolution ion microprobe (SHRIMP) U–Pb analyses of magmatic zircons derived from interflow chert (drillhole TD 1323, 214 m) high in the Paringa Basalt provided a date of 2690 ± 5 Ma (quoted in Connors et al., 2003; Clout, 1991).

Dolerite facies

The Defiance Dolerite occurs at the base of the Paringa Basalt and is up to 300 m thick, but is variable in thickness, being thin or absent in many areas of the camp (i.e. Intrepide to the Dome). The dolerite is distinctly zoned in areas where it is thick and well preserved. The unit is interpreted to have fractionated in situ to produce five internal zones:

- *Zone 1*: Directly overlies the Kapai Slate and has an average thickness of 55 m in the Victory mine area. It is an equigranular dolerite at the base, grading upwards into a medium-grained orthopyroxene orthocumulate with <10% feldspar. The bulk composition is about 18% MgO.
- *Zone 2*: Porphyritic dolerite consisting of glomero-porphyritic clusters of orthopyroxene altered to amphibole, in an equigranular pyroxene–plagioclase matrix.
- *Zone 3*: Equigranular dolerite with tabular plagioclase and lacking mafic phenocrysts. Granophyric intergrowths of albite and quartz comprise 10% of the groundmass, and form irregular patches up to 3 mm in diameter.
- *Zone 4*: Granophyric or oxide gabbro zone. It is defined by an increase in quartz-granophyre content to more than 10%, the presence of fine-grained subhedral magnetite, and the development of bladed pyroxene. Up to 70% spherulitic granophyre can be present in the centre.
- *Zone 5*: This is an upward gradation of Zone 4 into a medium- to fine-grained dolerite, which contains bladed ex-pyroxene with <10% granophyre. The upper chill zone contains radiating clusters of elongate branching pyroxene forming a quench texture.

The parental magma composition has been estimated by analysing chilled border zones and calculating the weighted average of all the internal zones. The interpreted parent magma composition is about 53% SiO_2 and 9.6–11.4% MgO, similar to the siliceous, high-Mg Paringa Basalt.

Black Flag Group

The contact between the Black Flag Group and the underlying Paringa Basalt is unconformable. The Black Flag Group consists of a lower sequence of mafic conglomerates, and felsic and intermediate volcanic rocks, and an upper sequence of felsic pyroclastic rocks and conglomerates, calcareous wackes, siltstones, and shales (McCall, 1969; Balkau, 1989). The sequences are called the Newtown Felsic Formation and the Morgans Island Epiclastic Formation, respectively.

Merougil Formation

The Merougil Formation outcrops on the west shores of Lake Lefroy, where it unconformably overlies the Black Flag Group. The formation is composed of lensoidal, monomictic to increasingly polymictic conglomerate units, and massive to stratified sandstones (Hand, 1996). The basal unconformity, which is typically faulted, marks a drastic change from a deep-water environment to a proximal braided river system. The formation is subdivided into a lower conglomerate-dominant facies and an upper sandstone-dominant facies (Bader, 1994).

Dolerites and gabbros

The stratigraphy is intruded by numerous mafic intrusions of varying thickness and displaying varying degrees of differentiation. Most are similar in geochemical composition to the lavas they intrude, and are therefore interpreted to be synvolcanic sills (e.g. Defiance Dolerite). However, the Junction and Condenser Dolerites are geochemically distinct from any known lavas in the area, and intrude the Black Flag Group.

The Condenser and Junction Dolerites are up to 500 m thick and are considered to be lateral equivalents of the very highly mineralized Golden Mile Dolerite at Kalgoorlie. They are internally zoned as follows:

- *Zone 1*: Weak pyroxene cumulate dominated by amphiboles and quartz, and containing less abundant feldspar. Ilmenite is the dominant oxide.
- *Zone 2*: Porphyritic dolerite containing amphiboles and an increased plagioclase content as distinct laths and an interstitial phase. Ilmenite and titanomagnetite are present.
- *Zone 3*: Quartz–plagioclase granophyre comprising up to 25% of the rock. Blue quartz is characteristic of this zone. Tabular plagioclase is common, and amphibole forms elongate acicular crystals. The oxide concentration is highest in this zone, consisting of co-existing ilmenite and magnetite.
- *Zone 4*: 'Bladed' dolerite with elongate to tabular amphiboles, and plagioclase as laths as well as an interstitial phase. Ilmenite is the dominant oxide.

Parental magma compositions are estimated by analysing chilled border zones or calculating the weighted average of all the internal zones. The Condenser and Junction Dolerites are Fe-rich tholeiites (50.6–51.1% SiO_2, 1.2–1.6% TiO_2, 12.7–14.5% FeO, and 5–7% MgO), very different in composition from the Defiance Dolerite (high-Mg basalt), but similar to the stratigraphically equivalent Golden Mile Dolerite. The Condenser and Junction Dolerites formed by the in situ differentiation of a tholeiitic magma. SHRIMP analyses of magmatic zircons from a pegmatite patch in the gabbro zone of the Condenser Dolerite gave a date of 2680 ± 8 Ma (Carey, 1994).

Granitoids

The Kalgoorlie and Black Flag Groups are intruded by intermediate to felsic granitoid stocks, dykes, and sills ranging from diorite to trondhjemite to rhyolite in composition (Roberts and Elias, 1990). Three major granitoid associations have been described:

1. Small intermediate to mafic intrusions that are aphyric and fine grained, deformed, and either bound by shear zones or forming layer-parallel bodies. A possible example is the Loreto Aplite (post D_1), dated at 2687 ± 4 Ma (quoted in Connors et al., 2003).

2. Large and subconcordant xenolithic sills, mainly of intermediate composition with rare felsic differentiates. Sills abound within the Kambalda Komatiite and are up to 300 m thick, possibly forming composite bodies; thinner felsic and intermediate sills intrude the Kapai Slate. The compositions of these rocks range from dioritic to granitic, with intermediate endmembers being hornblende phyric, and felsic members containing embayed quartz and albite phenocrysts in a fine-grained crystalline or glassy groundmass. SHRIMP analyses of magmatic zircons from a quartz–albite felsic porphyry at Victory gave an date of 2673 ± 10 Ma (Clout, 1991; quoted in Connors et al., 2003), whereas a xenolithic diorite and felsic phase from the Revenge mine yielded SHRIMP ages of 2661 ± 2 Ma and 2658 ± 4 Ma, respectively (Nguyen 1997).

3. Kambalda Granodiorite, a trondhjemite intrusion, and associated near vertical felsic dykes. These intrusions are largely massive, discordant to early structures, and are intruded along and deformed by late faults (Clark et al., 1986). The dykes are mainly felsic with quartz and albite phenocrysts, or rare megacrysts, in a glassy to medium-grained groundmass. The felsic dykes have equivocal field relationships with the Kambalda granodiorite. SHRIMP analyses of magmatic zircons from the Kambalda Granodoirite indicated a date of 2662 ± 6 Ma (drillhole LD9188/615, 624 m; Compston et al., 1986).

Four types of 'porphyry' intrusions are recognized in the Kambalda – St Ives area:

1. 'Pietra' porphyritic microgranodiorite, with 15–20% large rounded to lobate transparent quartz phenocrysts and about 25% smaller plagioclase phenocrysts, and hornblende bearing.

2. 'Lapis' porphyritic micromonzodiorite, with about 10% rounded to lobate transparent quartz phenocrysts and about 30% smaller plagioclase phenocrysts, and hornblende bearing.

3. 'Rocca' porphyritic micromonzodiorite, with 10–15% phenocrysts, most of which are feldspars, and lacking hornblende.

4. 'Flames' porphyritic tonalite to granodiorite, with quartz and albite phenocrysts, and alkali feldspar megacrysts. It also contains granite and lamprophyre xenoliths.

Geochemically, the granitoids are felsic to intermediate, with SiO_2 contents of 60–70%; $Na_2O + K_2O$ contents in the range 5–10%; and FeO/MgO ratios in the range 1.3–2.5. The rocks are classified as tonalite (dacite) and granodiorite or quartz-monzodiorite (trachydacite). Their major element compositions are the same, and they are sub-alkaline to calc-alkaline in geochemical affinity.

Lamprophyres

Lamprophyres are dark, strongly porphyritic, igneous intrusions that contain abundant euhedral phenocrysts of mafic minerals such as olivine, clinopyroxene, biotite or phlogopite, and amphibole, set in a felsic, mafic, or intermediate matrix. Important criteria for recognition are a lack of felsic phenocrysts, with feldspar and quartz being restricted to the groundmass. The principal types of lamprophyres in the Kambalda – St Ives area are kersantites and spessartites. SHRIMP analyses of magmatic zircons from kersantite bodies at Hunt and Cave Rocks (drillhole CVK166, 165 m) yielded dates of 2684 ± 6 Ma and 2627 ± 10 Ma, respectively (quoted in Connors et al., 2003).

Lamprophyres form a subordinate group of sills, dykes, and plugs in the Kambalda – St Ives district. Sills several metres thick intrude the Kapai Slate and thin biotite- and hornblende-phyric lamprophyre dykes have been identified associated with felsic dykes in the Lunnon shoot area and to the north of the Durkin shoot (Rock et al., 1990).

Geochemically, the lamprophyres are mafic to intermediate, with SiO_2 contents in the range 53–55%; $Fe_2O_{3\,total}$ contents of 6.3–7.4%; MgO content of of 7–9%; CaO content of 3–7%; and total volatiles in the range 4.0–8.5%. They are enriched in large-ion lithophile elements, with K_2O contents of 1.33–2.7%; Rb contents of 56–83 ppm; and Ba contents of 885–1296 ppm. Most of the incompatible elements, such as Th, Zr, P, and light rare earth elements (LREE), are also enriched relative to mid-ocean ridge basalt (MORB). Compatible elements Cr and Ni are present in moderate to high amounts.

Proterozoic dykes

Unmetamorphosed Proterozoic dolerite dykes intrude fracture sets with four main orientations: east, northeast, east-northeast, and south-southeast. The dykes are subvertical and up to 40 m thick. Proterozoic dykes are distinguished from Archaean dolerites by the presence of olivine, a strongly magnetic character, and abundant epidote on fracture surfaces.

Tectonostratigraphic evolution

The stratigraphic sequence shows the effects of four phases of post-volcanic compressional deformation (D_1–D_4), and a number of deformation schemes have been proposed. More recent interpretations of the structural history have recognized the importance of several episodes of extensional deformation and basin formation in the development of the early fault architecture, which, in turn, has had a significant influence on the later history of compressional deformation.

Nguyen (1997) recognized the same four major compressional events as previous workers, but also included an early episode of basin development during formation of the Kambalda stratigraphy (D_{e1}), and an early D_3 stage of northeasterly to east-northeasterly subhorizontal extension associated with deposition of the Merougil Formation and emplacement of quartz–albite dykes. More recent geochronology suggests that the Merougil Formation was deposited during the later stages of D_2 compression (see below), and that the extension event noted by Nguyen (1997) probably occurred between D_1 and D_2 (D_{e3} in Table 2, rather than between D_2 and D_3). Workers in other parts of the Yilgarn Craton have recognized an additional period of extensional deformation (D_{e2} in Table 2, Fig. 5) between the two noted by Nguyen (1997), and this is associated with felsic magmatism, and Black Flag Group sedimentation and volcanism. Seismic data suggest that some structures, such as the Abbatoir Shear, were active during this event.

D_{e1} mafic–ultramafic volcanism

The tectono-stratigraphic history of the Eastern Goldfield Province started with a period of mafic–ultramafic volcanism (D_{e1}) at 2720–2690 Ma (Barley et al., 2002). The mafic to ultramafic volcanic rocks were deposited in basins formed within older continental crust, which appears to be largely felsic, based on the seismic reflection data and gravity modelling (Goleby et al., 1993). This older crust is locally exposed at the southern end of the Eastern Goldfield Province at Norseman, where the rocks have been dated at c. 2930 Ma (Hill et al., 1992). The stratigraphic units in the St Ives area that formed during this period are collectively termed the Kalgoorlie Group and include the:
- Lunnon Basalt;
- Kambalda Komatiite (2709 ± 4 Ma, U–Pb zircon SHRIMP; Claoué-Long et al., 1988);
- Devon Consols Basalt (2693 ± 30 Ma, U–Pb zircon SHRIMP; Compston et al., 1986);
- Kapai Slate (2692 ± 4 Ma, U–Pb zircon SHRIMP; Claoué-Long et al., 1988);
- Defiance Dolerite;
- Paringa Basalt (2690 ± 5 Ma, U–Pb zircon SHRIMP; Clout, 1991).

The faults that originated during this deformation event are interpreted to include many of the major north-northwesterly trending structures previously interpreted as being D_3. Significant across-structure stratigraphy variations indicate that these structures were probably involved in basin development during this event.

D_{e2} felsic magmatism

The second major depositional event (D_{e2}) occurred from c. 2690 to 2660 Ma (Barley et al., 2002), involved north-northwesterly–south-southeasterly extension (based on extensional fabrics in c. 2680 Ma granitoid domes; Williams and Whitaker, 1993), and was associated with felsic magmatism, sedimentation, and local mafic magmatism (Condenser, Defiance, and Junction Dolerites; 2680 ± 8 Ma). This event resulted in deposition of the

Table 2. Compilation of the deformation history for Kambalda region. See text for references

Deformation event	*Major features*	*Orientation*	*Approximate age (Ma)*
D_{e1}	Mafic–ultramafic volcanism	Approximately east–west 'extension'	2720–2690
D_{e2}	Felsic magmatism, Black Flag sedimentation	North-northwest–south-southeast extension with southeast side down	2690–2660
D_1	Thrust faults, major stratigraphic repetitions; ?gold at Golden Mile (pre-D_2)	North–south shortening	c. 2660
D_{2a}	Folds and cleavage (early D_2 folds cut by late basins, e.g. Kurrawang and Pig Well)	East-northeast–west-southwest shortening	unknown
D_{e3}	Late Basin sedimentation (Merougil); felsic magmatism (switch high Ca to low Ca)	Approximately northeast–southwest extension in strike slip setting	<2657
D_{2b}	Folds and thrust faults; Au at Wallaby c. 2650 Ma (post late basins, but early D_{2b})	East-northeast–west-southwest shortening	c. 2650–2645
D_{2x}[(a)]	Structures in granites, minor northeasterly trending folds overprinting D_2 northwesterly trending folds, reactivation of D_1 thrusts with possible development of new thrust faults	Approximately northwest–southeast shortening	c. ?2645
D_3	Folds and faults; gold at St Ives (dated at 2631 ±5 Ma and 2627 ± 7 Ma)	East-southeast–west-northwest shortening	c. ?2645–2630
D_4	Northeasterly to northerly trending faults, reactivation of earlier faults	Northeast–southwest shortening	c. 2630–2625

NOTE: (a) Geoscience Australia work: Blewett et al. (2004)

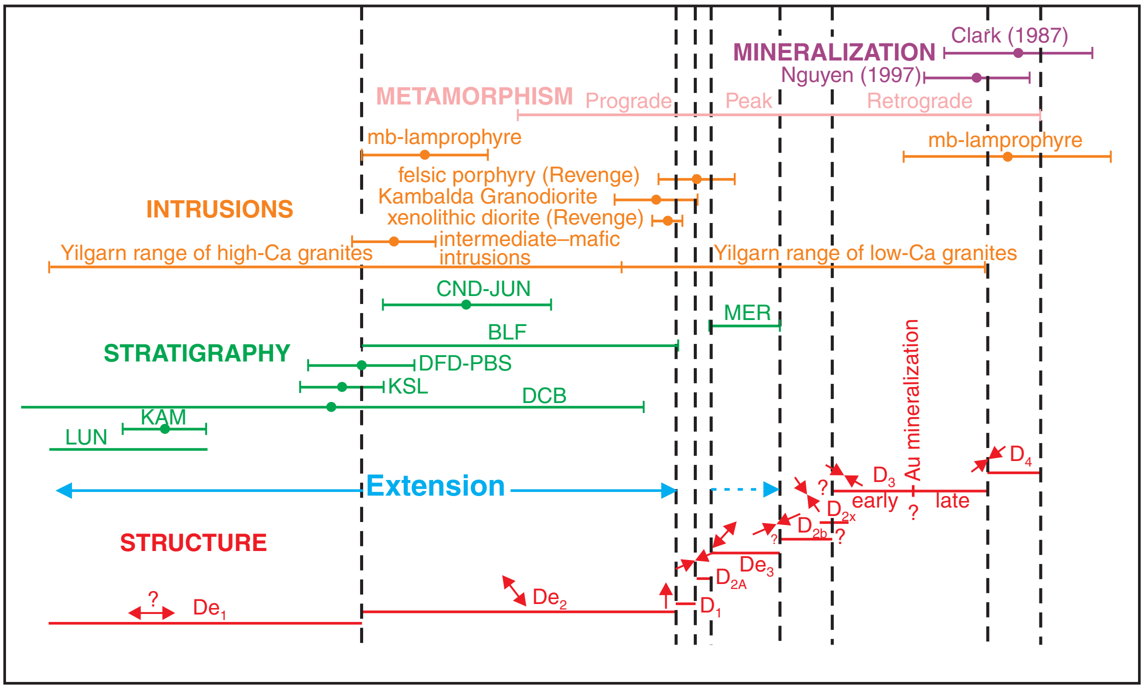

Figure 5. Temporal and structural framework for the Kambalda–Tramways corridor. BLF = Black Flag Group, CND–JUN = Condenser and Junction Dolerites, DCB = Devon Consols Basalt, DFD–PBS = Defiance Dolerite and Paringa Basalt, KAM = Kambalda Komatiite, KSL = Kapai Slate, LUN = Lunnon Basalt, MER = Merougil Formation, mb-lamprophyre = biotite lamprophyre

extensive Black Flag Group. The basins related to this stage of extension generally deepen to the south, implying southeast-side-down displacement (Hayward, N., 2001, pers. comm.). Intrepretation of seismic data in the St Ives area suggests that the Boulder–Lefroy Fault dips east and formed as an extensional fault during deposition of the Black Flag sequence.

D_1 north–south thrusting

D_{e2} sedimentation and felsic magmatism were followed closely by D_1 thrust faulting at c. 2657 Ma, which involved north–south compression and inverted the basins developed during D_{e2}. This event resulted in development of westerly trending thrust faults, and recumbent folds. Some of the best-documented D_1 thrusts within the Yilgarn Craton occur in the St Ives area, including the Foster, Tramways, and Republican Thrusts. Swager and Griffin (1990) interpreted these thrust faults as part of a megaduplex, which formed in response to northwards thrusting and could have linked into the Feysville Thrust. Other well-documented D_1 thrusts occur in the Kanowna and Dunnsville areas.

D_{2a} east-northeasterly–west-southwesterly shortening

Early north-northwesterly trending D_{2a} folds are truncated by the late basins (D_{e3} sedimentation) in both the Pig Well (Blewett et al., in press) and Kurrawang areas. This implies that a stage of east-northeasterly–west-southwesterly shortening had initiated prior to the extensional event related to deposition of the late basins.

D_{e3} late basin sedimentation and felsic magmatism

A third major depositional event occurred post c. 2655 ± Ma, based on the youngest zircons found in any of the late basins (Krapez et al., 2000). However, the ages of these basins vary across the Eastern Goldfield Province (Blewett et al., in press). Age dating in the St Ives area suggests that the widespread felsic to intermediate porphyries and the Kambalda Granodiorite were emplaced during or just before this event. The Kambalda Granodiorite, which is exposed in the dome area, has been dated at 2662 ± 4 Ma (U–Pb zircon SHRIMP; Compston et al., 1986), whereas the porphyries have been dated at 2660 ± 6 Ma and 2658 ± 4 Ma (U–Pb zircon SHRIMP; Nguyen, 1997), and 2680 ± 12 Ma (U–Pb zircon; Clark, 1987). There are few data to indicate the extension direction during this event but, given the dominant northwesterly–southeasterly trend of the porphyries in much of the St Ives area, it is considered most likely that the extension direction was about northeast–southwest.

The fluvial rocks of late basins such as the Merougil Formation (and equivalents including Jones Creek Conglomerate and Yandal Sandstone) are interpreted to have been deposited in elongate, localized basins, in contrast to the widespread turbidite fan deposits of the Kurrawang Formation (Barley et al., 2002).

D_{2b} main stage of east-northeasterly–west-southwesterly shortening

D_{2b} east-northeasterly–west-southwesterly shortening is interpreted to have occurred late syn- to post-granite intrusion (Archibald, 1985; Nguyen, 1997) at c. 2650 Ma or later. This event represents the major period of crustal shortening within the Eastern Goldfield Province, and is readily recognized throughout the Yilgarn Craton, including the Southern Cross Province. D_2 shortening is associated with large-scale north-northwesterly trending folds and abundant north-northwesterly trending thrust faults. This event resulted in inversion of the extensive basins of mafic–ultramafic rocks that developed during D_{e1}. Peak metamorphic conditions are interpreted to have been reached broadly synchronous with D_2 in the St Ives region (Archibald, 1985; Nguyen, 1997). However, it has been suggested that peak conditions were reached at a later time at depth (Hayward, N., 2001, pers. comm.). If this is the case, then it allows for the involvement of metamorphic fluids in D_3 mineralization.

D_2 involved the generation of open upright folds such as the Kambalda and Widgiemooltha Domes, the development of the main upright cleavage (S_2 foliation), and M_2 greenschist metamorphism, possibly synchronous with the main phase of granitoid intrusion. The D_2 folds are roughly parallel with the major north-northwesterly striking fault systems of the Yilgarn Craton, but most of these faults, such as the Boulder–Lefroy Fault and Zuleika Shear, are interpreted to have formed during earlier D_{e1} or D_{e2} extensional deformation. At a regional scale, the folds are components of large north-northwesterly trending anticlinoria (Kalgoorlie – Kambalda – St Ives and Depot Rocks – Widgiemooltha – Pioneer corridors) and synclinoria (Kurrawang and Merougil Basins). In the seismic studies of Goleby (1993) and Williams (1993), the regional anticlinoria and synclinoria appear as openly folded, imbricately stacked wedges bounded by north-northwesterly striking anastomosing faults, which could be stacked listric thrusts and backthrusts linked in a flat basal decollement at 6 km depth.

Regional S_2 foliations are defined by peak metamorphic mineral assemblages, which indicate that peak regional metamorphism accompanied this phase of crustal shortening and thickening. In addition, many of the elongate, foliated syntectonic granitoid plutons are interpreted to have intruded into anticlinal hinge zones at this time. The occurrence of telescoped metamorphic grade changes across D_2 faults (Archibald, 1979; Hayward, 1988) and the abundance of retrogressive chlorite–calcite alteration halos around them suggest D_2 thrusts remained active following peak metamorphism. The general lack of economic gold mineralization associated with D_2 thrusts suggests that the post-peak metamorphic carbonation event considered by many to be intimately associated with gold mineralization actually predates mineralization (Bennet, 1995).

D_{2x} northwest–southeast shortening

Recently, workers from Geoscience Australia have documented evidence for a period of northwesterly–southeasterly shortening after D_2 and before D_3 (Blewett et al., 2004). The main lines of evidence for this event are:

- the results of a detailed study of granitoids in the Laverton area showing the presence of structures related to this event;
- minor 'refolding' of northwesterly oriented D_2 folds by northeasterly oriented folds, resulting in variations in plunge direction;
- some 'D_1' thrusts at St Ives and Kanowna Belle appear to cut D_2 folds and are not folded by this event, as previously interpreted;
- the D_1 Republican thrust at St Ives cuts a northwesterly trending fault, which, in turn, cuts the major Boulder–Lefroy Fault.

At present it is uncertain whether D_1 thrusts have simply been reactivated during the D_{2x} northwest–southeast shortening event, or whether the faults originated at this time.

D_3 east-southeast–west-northwest shortening

D_3 east-southeast–west-northwest shortening represents a return to the broadly east–west shortening direction of D_2. The east-southeast–west-northwest shortening direction for the St Ives area is confirmed by sinistral reverse movement on numerous northerly trending faults, in contrast to the east-northeast–west-southwest D_3 shortening direction in the Kalgoorlie area. D_3 deformation resulted in the tightening of D_2 folds and local development of new folds overprinting D_2 structures, as well as reactivation of old faults and development of new faults, largely as subsidiary structures to the pre-existing north- to northwesterly trending faults. The timing of the change from east-northeast to east-southeast shortening is not well constrained, but is likely to have been c. 2645 Ma (or later).

The later stages of D_3 east-southeast–west-northwest shortening, which coincided with gold mineralization at St Ives, must have pre-dated 2632 Ma, the age of a post-tectonic granite cutting the Ida Fault (Bateman, 2001). This age represents a minimum age for any major deformation including D_4. Age dating at St Ives suggests that the Victory and Revenge gold mineralization formed during the final stages of D_3 deformation.

D_4 shortening

D_4 deformation is generally interpreted as northeast–southwest shortening that resulted in reactivation of various faults and development of brittle northeasterly and northwesterly trending faults (Nguyen, 1997). In general, this event does not appear to be very significant but it could be associated with the final stages of mineralization. At St Ives, the Redoubtable deposit has been interpreted as synchronous with D_4 deformation, given that it is associated with the Alpha Island Fault, which has been considered to be D_4 in age. However, observations during this study suggest that the fault is older.

Metamorphic setting

The style of metamorphism at Kambalda appears to be static, with good preservation of volcanic textures. Peak metamorphic conditions during D_2 ranged from upper greenschist to lower amphibolite facies in the Kambalda Dome, to mid-amphibolite facies in the Widgiemooltha and Carnilya Hill areas (Bavinton, 1979; Archibald, 1985; Perriam, 1985; Goodgame, 1997). Peak metamorphic conditions are estimated at 520 ± 20°C and 1–4 kbar in the St Ives camp (Bavinton, 1979; Donaldson, 1983; Archibald, 1985). Higher metamorphic temperatures were reached in the contact aureole of the Kambalda Granodiorite (Wong, 1986). Retrograde greenschist facies metamorphism extended from D_3 to D_4.

Camp- to deposit-scale hydrothermal alteration footprints

Camp-scale hydrothermal alteration zonation

In the St Ives camp, a range of alteration styles is documented (Clark, 1987; Neall and Phillips, 1988; Clark et al., 1989; Nguyen, 1997; Polito et al., 2001; Neumayr et al., 2003). The alteration styles are the result of several metasomatic events related to different deformation events, and are telescoped. Documented styles are:

1. carbonate associated with deformation along the transcrustal structure (Lefroy);
2. epidote–calcite–magnetite–pyrite–chalcopyrite–quartz,
3. magnetite halo around gold-bearing structures (interpreted as oxidized hydrothermal fluid);
4. pyrrhotite(–pyrite) alteration flanking oxidized domains on a camp scale (interpreted as reduced hydrothermal fluid);
5. zoned chlorite–biotite–feldspar–carbonate–pyrite quartz alteration associated with gold.

For gold mineralization, styles 3, 4, and 5 are the most important, and are discussed here in more detail.

Gold-associated sulfide and oxide minerals indicate a zonation with respect to ore-fluid chemistry within the St Ives gold camp (Fig. 2). Oxide and sulfide assemblages are correlated to reduced and oxidized conditions using fO_2–$\alpha\Sigma S$ diagrams at 400°C and 2 kbar. Deposits in the southwest of the camp, such as Argo and Junction, contain arsenopyrite–pyrrhotite and pyrrhotite–pyrite assemblages, respectively. These assemblages indicate dominant relatively reduced hydrothermal fluids. The deposits in the 'central corridor' of the St Ives gold camp are characterized by pyrite–magnetite and pyrite–hematite assemblages, indicating dominant relatively oxidized hydrothermal fluids. Deposits in the northwest, close to the Kambalda dome, typically contain pyrite as the main sulfide mineral.

In the central corridor, two main domains are distinguished with respect to the redox conditions of the hydrothermal alteration (Fig. 6; Neumayr et al., 2003):

- reduced (pyrrhotite–pyrite and pyrrhotite assemblages);
- oxidized (pyrite–magnetite and pyrite–hematite assemblages).

The domain mapping is not completed as yet, but preliminary data indicate a distinct distribution pattern. Domains with oxidized alteration assemblages are focused, and are best mapped by hydrothermal magnetite in sedimentary rocks, such as the Kapai Slate. Magnetite in Kapai Slate is present around the Victory–Defiance deposits and to the southeast of, and locally within, the Greater Revenge area. These domains with magnetite–pyrite assemblages are aligned along some major structures, such as the northwesterly trending, northeasterly dipping Playa fault, and domains with magnetite–pyrite also rim two pronounced gravity lows centred around the Victory–Defiance deposits, and to the west of the Revenge deposits (Fig. 7). The gravity lows extend for several kilometres in diameter, and are interpreted to represent abundant magmatic intrusions at a depth of about 500–1000 m below present surface. Abundant felsic intrusions are also interpreted from seismic data in a cross section across Victory–Defiance (Fig. 8). Domains with reduced alteration assemblages (pyrrhotite–pyrite) flank those with oxidized assemblages to the northeast and southwest of the Victory–Defiance and Greater Revenge deposits. and are also present locally between oxidized domains in the Greater Revenge deposits.

Deposit-scale hydrothermal alteration in oxidized deposits

At a deposit scale, hydrothermal alteration mineralogy depends mainly on the host rock composition. Therefore, any comparison of hydrothermal alteration between deposits has to take into account the host rock types. Hydrothermal alteration is discussed here mainly for mafic host rocks, as exemplified by the Revenge and Conqueror gold deposits. In the Conqueror deposit, most distal hydrothermal alteration assemblages are pyrrhotite–pyrite. Gold lodes are rimmed by a >100 m-wide halo of hydrothermal, fine-grained magnetite, which is best monitored via variations in the magnetic susceptibility. However, the gold lodes themselves are characterized by low magnetic susceptibility and less abundant magnetite. Hydrothermal magnetite proximal to gold lodes is overprinted by the typical zoned gold-associated alteration (chlorite, chlorite–biotite, and feldspar–carbonate–pyrite). The most distal zone of gold-associated alteration contains hydrothermal chlorite, and less abundant biotite and dolomite (Clark et al., 1989; Neumayr et al., 2003). The intermediate alteration zone, proximal to the gold lodes, comprises hydrothermal biotite, carbonate, and lesser albite and pyrite, with traces of magnetite. The most proximal areas to the gold lodes are bleached zones adjacent to hydrothermal quartz veins, and these contain albite, ankerite, dolomite, quartz, and pyrite, as well as less abundant biotite, muscovite, and calcite. Gold-associated pyrite grains contain magnetite inclusions in their cores and hematite inclusions in their rims.

Deposit-scale hydrothermal alteration in reduced deposits

Both reduced deposits in the camp (Argo and Junction) are hosted in dolerite near the contact of the mafic succession and the Black Flag Group. Three distinct

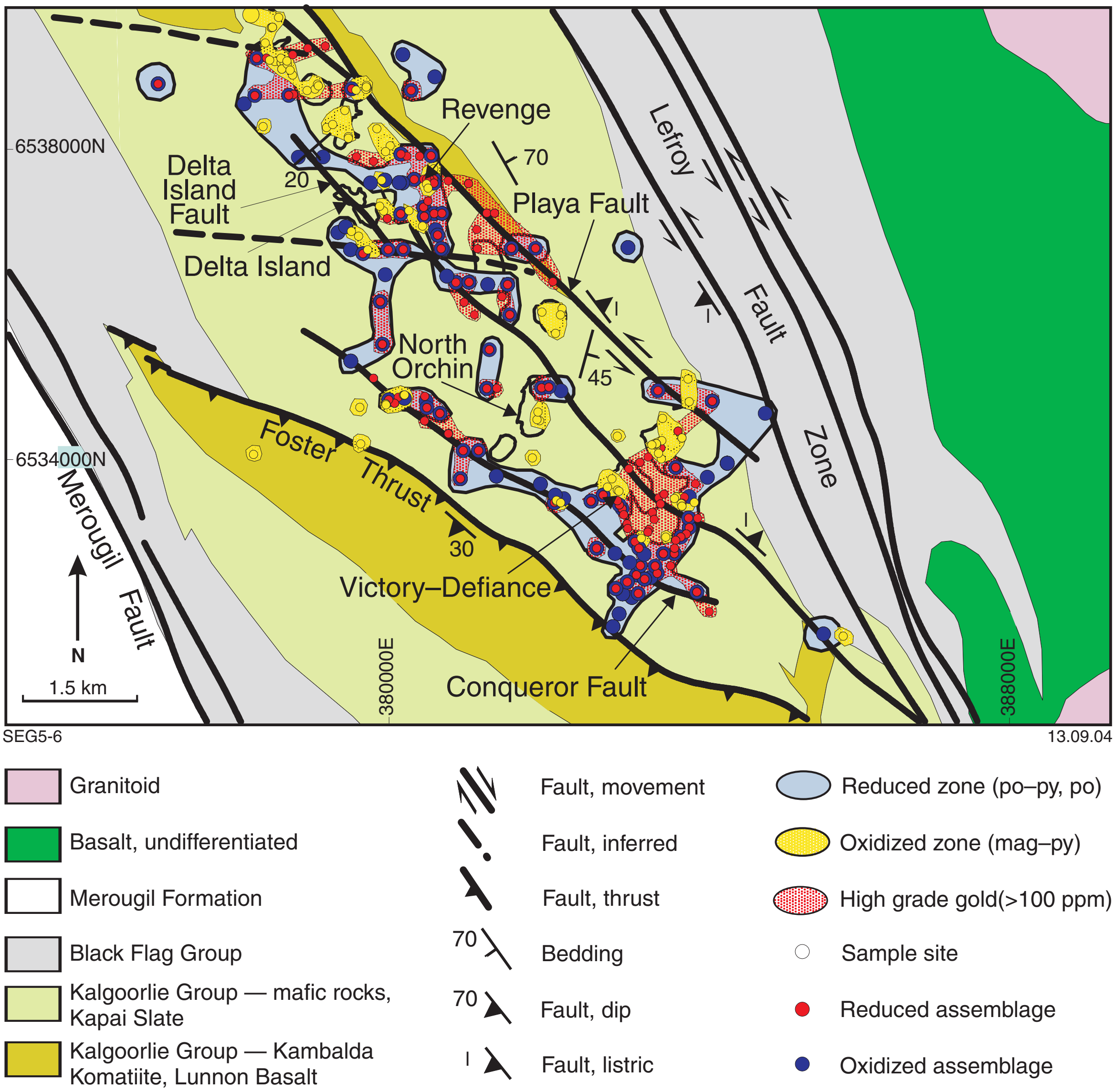

Figure 6. **Simplified geology, main deposits, and redox mineral assemblages in the St Ives gold camp. The figure shows the main distribution of reduced (pyrrhotite–pyrite) and oxidized (magnetite–pyrite) assemblages in the camp. Note that high grade (>100 ppm) gold intersections are located at the boundary between reduced and oxidized domains**

mineralization styles contribute to gold mineralization at the Argo A1 orebody. The first is represented by the intensely sheared mylonite, which has three distinct alteration halos:

- the distal alteration halo is defined by a chlorite–calcite–pyrrhotite assemblage;
- the intermediate alteration zone is characterized by the assemblage biotite–chlorite–plagioclase;
- proximal alteration zone is reflected by the increased modal abundance of albite–quartz(–dolomite or ankerite).

The sulfide assemblage in the proximal zone is pyrrhotite–arsenopyrite–chalcopyrite–pyrite. The main development of alteration halos is replaced in the centre of the proximal zone by the reactivation and subsequent brecciation. Late brittle quartz-rich veins overprint the mylonitic shear zone and the breccia.

Controls on gold mineralization

Host rock controls

Gold mineralization in the St Ives camp can be subdivided into three distinct types with respect to their host rocks. The Junction group comprises two main deposits: Junction and Argo. These deposits are hosted by the Condenser and Junction Dolerites.

Gold deposits in the Victory–Defiance complex are hosted in several rock types, including Kambalda Komatiite, Paringa Basalt and Defiance Dolerite, Flames porphyry, and Kapai Slate. The Intrepide deposit group includes two main deposits, Intrepide and Redoubtable, and an old working mine, Red Hill. These deposits are mainly associated with porphyry–ultramafic contacts.

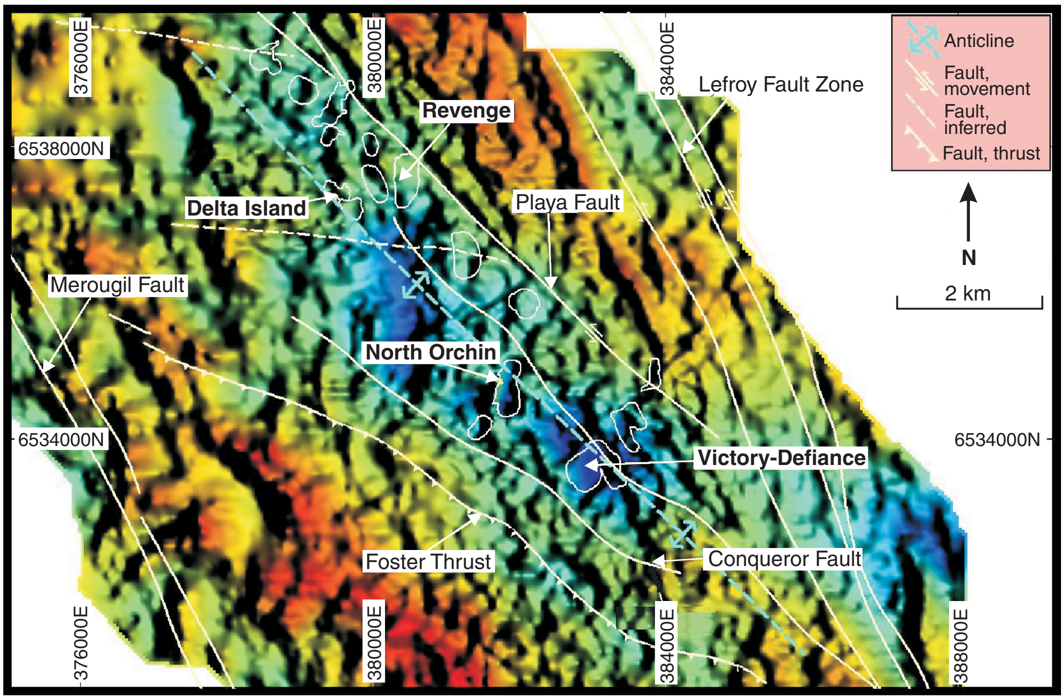

Figure 7. Detailed gravity image of the St Ives gold camp showing main structures and location of gold deposits. Note the distinct gravity lows in the Victory–Defiance area and southwest of the Revenge deposit

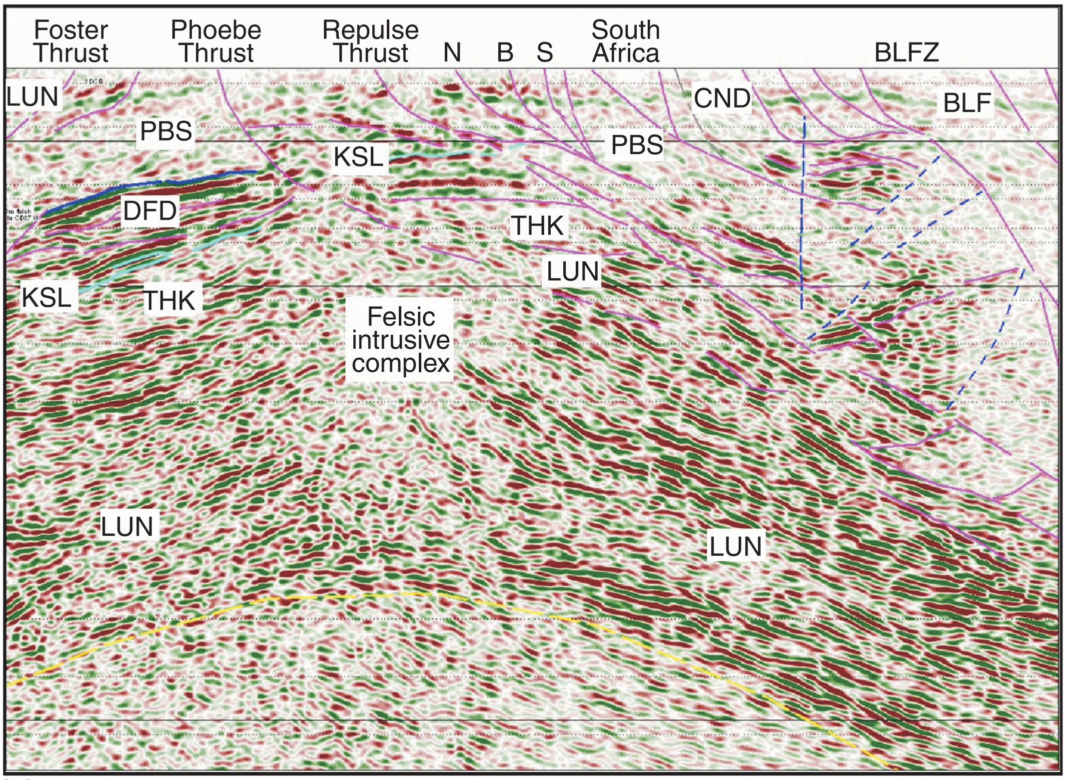

Figure 8. Seismic cross section across the Victory–Defiance gold deposits. The image shows main rock types and structures. Note the seismic response and location of the felsic intrusive complex beneath Victory–Defiance. B = Britannia Thrust, BLFZ = Boulder–Lefroy Fault Zone, N = Nautilus Thrust, S = Sirius Thrust, THK = Tripod Hill Komatiite. Other abbreviations as in Figure 5

Shearing is controlled by the mechanical contrast between brittle porphyry and ductile ultramafic rocks. The ultramafic rocks are typically foliated whereas quartz vein stockworks are developed in the porphyry.

Dolerite, including the Defiance and Junction Dolerites, is currently considered the most favourable host rock for the St Ives camp because it hosts the largest gold deposits (Junction, Defiance, Revenge, Argo, Conqueror, Orchin, North Orchin), and accounts for about 70% of pre-mining reserves (Roberts and Elias, 1990; Nguyen et al., 1992), although this could change with recent and current drilling in the Revenge complex. High-grade gold mineralization is mainly associated with thick magnetite-rich granophyric zones of the dolerite (Nguyen, 1997). Basalt, including the Lunnon, Devon Consols, and Paringa Basalts, currently accounts for about 20% of the pre-mining reserves. The magnetite-bearing chert facies within the Kapai Slate typically hosts high grade but low tonnage orebodies. Felsic intrusions are commonly poorly endowed but, adjacent to ultramafic rocks, the competency contrast between brittle felsic and ductile ultramafic rocks has localized gold mineralization (Intrepide, Redoubtable, and Formidable).

Structural controls

The following description of the structural controls on gold mineralization in the St Ives camp is summarized from Cox and Ruming (2004). Gold mineralization at St Ives formed during D_3. Many of the gold deposits are hosted by faults and shear zones that are spatially and kinematically related to D_3 displacement on the Playa Fault (Fig. 9). These deposits occur in low displacement brittle–ductile shear zones, which are interpreted as splays and linked fault–shear networks in a 2 km-wide zone west of the Playa Fault (Figs 9 and 10). The total displacement on the northwesterly trending Playa Fault is poorly constrained, but could be up to several kilometres.

In contrast, ore-hosting structures in individual deposits such as Revenge, North Orchin, Argo, and much of the Victory area, are mainly northerly striking, moderately to gently east- or west-dipping reverse faults and shear zones with maximum displacements of a few tens of metres. Strike lengths of ore-hosting structures are rarely more than about 1 km. The orientations of stretching lineations, curvature of shear zone foliations, associated gently dipping extension veins, and stratigraphic separations all indicate a reverse slip sense for most D_3 ore-hosting structures, especially in the Argo–Victory–Revenge area. The geometries of faults and associated extension veins indicate formation in a stress regime in which the far-field maximum principal stress was approximately east–west and horizontal.

In the Victory–Defiance area, ore is localized along an apparently imbricate series of moderately to gently dipping, low displacement thrusts. The Playa Fault here (known locally as the Repulse Fault in the Victory–Defiance mine area) has a ramp–flat–ramp geometry. Where it is more gently dipping, a number of low displacement, ore-hosting thrusts splay from the Playa Fault into its hangingwall. To the west, where the Playa Fault forms a more steeply dipping ramp, low displacement, ore-hosting thrusts occur in the footwall of the Playa (Repulse) Fault, and host the Defiance and Conqueror lodes. The geometry and kinematics of the Victory thrust complex, and its geometric relationship with the Playa Fault indicate that the thrust complex developed within a jog on the Playa Fault, to the northwest of where it splays from the Boulder–Lefroy Fault. The overall northwesterly trend and predominantly sinistral shear sense on the Playa Fault, as well as the thrust to oblique-thrust sinistral shear sense on low displacement faults within the imbricate thrust complex, are interpreted to indicate that gold mineralization here is localized within a kilometre-scale contractional jog that was active during D_3, and the contemporaneous hydrothermal alteration and gold mineralization.

Similarly, the orientation and reverse shear sense of the low displacement, ore-hosting structures on the western side of the Playa Fault, for more than 5 km northwest of the jog (Victory–Revenge area), are also interpreted as contractional structures (Cox and Ruming, 2004), whose formation is kinematically related to mainly sinistral slip on the Playa Fault during D_3. Accordingly, the gold deposits in the Orchin to Revenge areas are interpreted to have formed in a low displacement contractional damage zone generated by strain accommodation around the Victory jog (Figs 10 and 11). Northwest of the Revenge area, several gold deposits and prospects occur within the Playa Fault, or west of this structure.

The Delta and Santa Ana deposits are localized in northwesterly trending fault zones west of the Playa Fault. The Formidable, Redoubtable, and Intrepide deposits are located within the Playa Fault, or strands of this structure. The Minotaur, Mars, and Agamemnon deposits are associated with shear zones that are likely to be link structures between the Playa Fault and the Delta Fault north of the Delta deposit.

The Argo and Junction deposits are spatially separated from the other St Ives deposits, and located south of the Victory jog and west of the Boulder–Lefroy Fault. Argo occurs within a moderately westerly dipping, brittle–ductile, reverse shear zone. The Junction deposit is located along an easterly dipping, north-northwesterly trending, reverse or sinistral shear zone. Maximum displacement on these latter structures is between 50 and 100 m.

Displacement on ore-hosting structures in the St Ives goldfield involved both ductile and brittle processes. Hydrothermal alteration and associated gold mineralization were synchronous with deformation along the ore-hosting network of shear zones. In many deposits, ductile shearing was punctuated by repeated brittle slip events, which produced breccias and shear veins, especially in jogs and dilatant bends in shear zones.

By analogy with modern seismogenic systems, the low displacement structures that localized fluid flow and gold mineralization in the St Ives goldfield are interpreted by Cox and Ruming (2004) as aftershock structures whose development and distribution was controlled by major slip events on the Lefroy Fault. For a number of years, seismologists have been successfully using analysis of

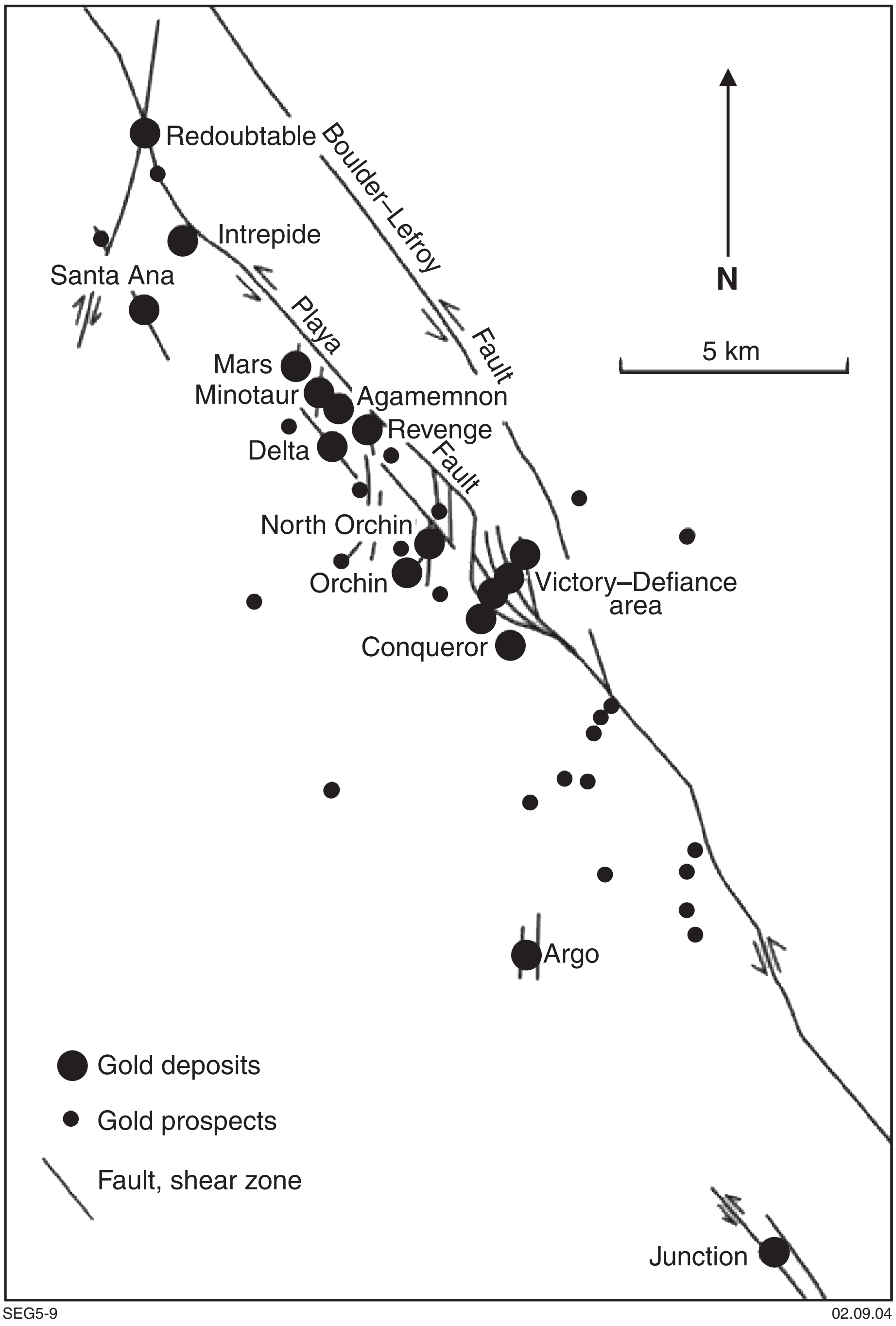

Figure 9. Simplified map illustrating the geometry and distribution of D_3-active faults and shear zones, including the Boulder–Lefroy Fault, the Playa Fault and various lode-hosting faults in the Kambalda region (modified after Cox and Ruming, 2004). Major gold deposits in the St Ives goldfield are also shown

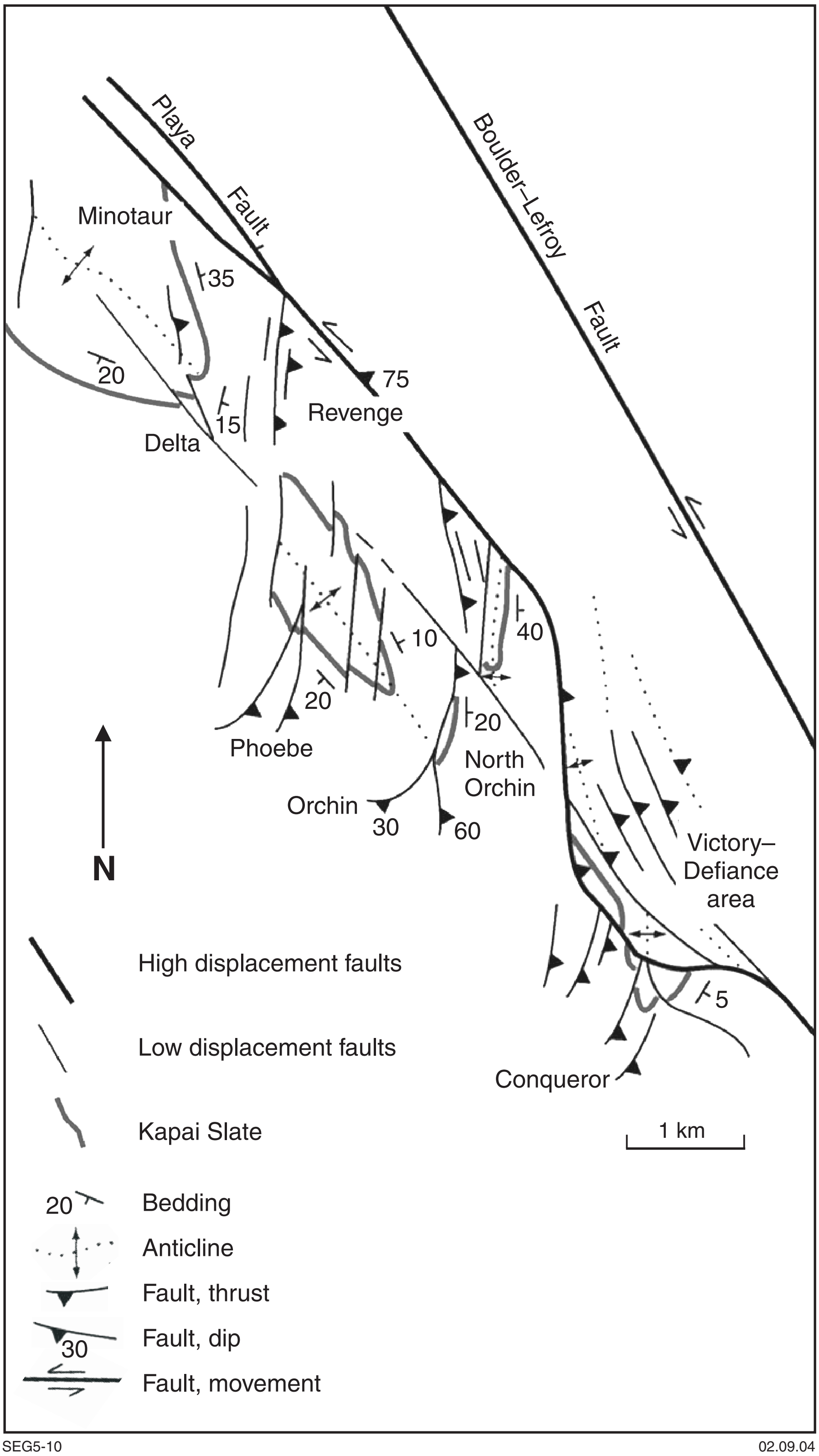

Figure 10. Fault geometry and distribution in the central part of the St Ives goldfield (modified after Cox and Ruming, 2004). The deposits of the Victory–Defiance area are located in an imbricate thrust complex developed within a contractional jog on the largely sinistral Playa Fault. Other deposits are localized mainly on northerly trending reverse faults in a contractional domain northwest of the Victory jog

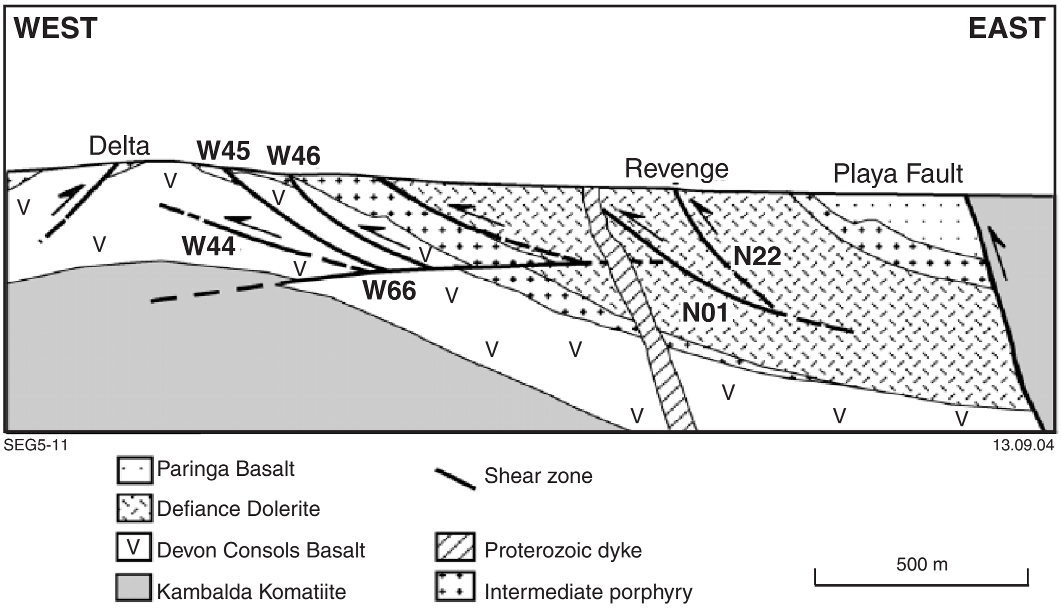

Figure 11. Simplified east–west cross section of the Revenge mine area. Orebodies (numbered) are hosted in conjugate thrusts just west of the Playa Fault (after Nguyen et al., 1998)

stress changes induced by mainshock earthquake ruptures (stress transfer modelling) to predict where, in active fault systems, aftershocks are most likely to occur. On this basis, Cox and Ruming (2004) have used stress transfer modelling to test if the location of the St Ives goldfield within the Boulder–Lefroy Fault has a relationship to the structure of the fault system.

It was found that, for large slip events (magnitude 6.5) on the Lefroy Fault, the predicted aftershock footprint produced by mainshock rupture arrest at the Victory jog very closely matches the location and geometry of the St Ives goldfield. The modelling supports an interpretation that aftershock networks can form a high permeability damage zone that localizes fluid flow and gold mineralization within particular parts of crustal-scale fault systems. The aftershock concept provides one explanation for the long-known relationship that gold deposits hosted by faults or shear zones tend to occur in low displacement structures up to several kilometres from the associated crustal-scale shear zones.

Both co-seismic stress transfer and time-dependent changes in fluid pressures, during post-seismic fluid redistribution, are implicated in driving the growth of low displacement, gold-hosting fault networks in the St Ives goldfield. Stress transfer modelling can be applied to area selection in exploration programs targeting mesothermal gold systems. Clustering of deposits hosted by aftershock fracture networks is favoured by the presence of major, long-lived jogs or bends, which can repeatedly arrest ruptures propagating along high displacement faults.

Chemical controls

Chemical controls are described for the oxidized deposit groups because these are the best documented to date (Clark et al., 1989; Neumayr et al., 2003). Whereas Clark et al. (1989) documented conditions of hydrothermal alteration and chemical changes during alteration, recent camp-scale studies identified camp-scale hydrothermal alteration footprints and distinct chemical controls on the location of high-grade gold mineralization (Neumayr et al., 2003).

On a camp scale, two main domains of sulfide–oxide mineral assemblages (pyrrhotite–pyrite, magnetite–pyrite) are identified and are best interpreted to relate to two hydrothermal fluids, one a reduced system and the other oxidized, respectively (Neumayr et al., 2003). Oxidized mineral assemblages, as well as felsic to intermediate porphyry intrusions, are centred around the Greater Revenge and Victory–Defiance mines. This suggests that oxidized mineral assemblages are genetically related to the porphyry intrusions. Reduced mineral assemblages are located outboard of the oxidized domains, and flank these domains to the northeast and southwest. High grade (>100 ppm) gold intersections are preferentially located at the border, or in overlapping zones, between reduced and oxidized domains, but within the oxidized domain (Figs 6 and 12). This indicates a chemical control on the precipitation of high-grade gold mineralization.

Currently, there are two competing genetic models to explain the oxide–sulfide mineral assemblage. The first model assumes that two hydrothermal fluids of different redox state infiltrated the rock volume progressively. The second fluid interacted with hydrothermal alteration that had precipitated from the earlier fluid. Large differentials in the redox state between the new fluid and alteration from the first fluid provided a powerful gold precipitation mechanism.

In the second model, interaction of two contemporaneous fluids of grossly different redox state is assumed.

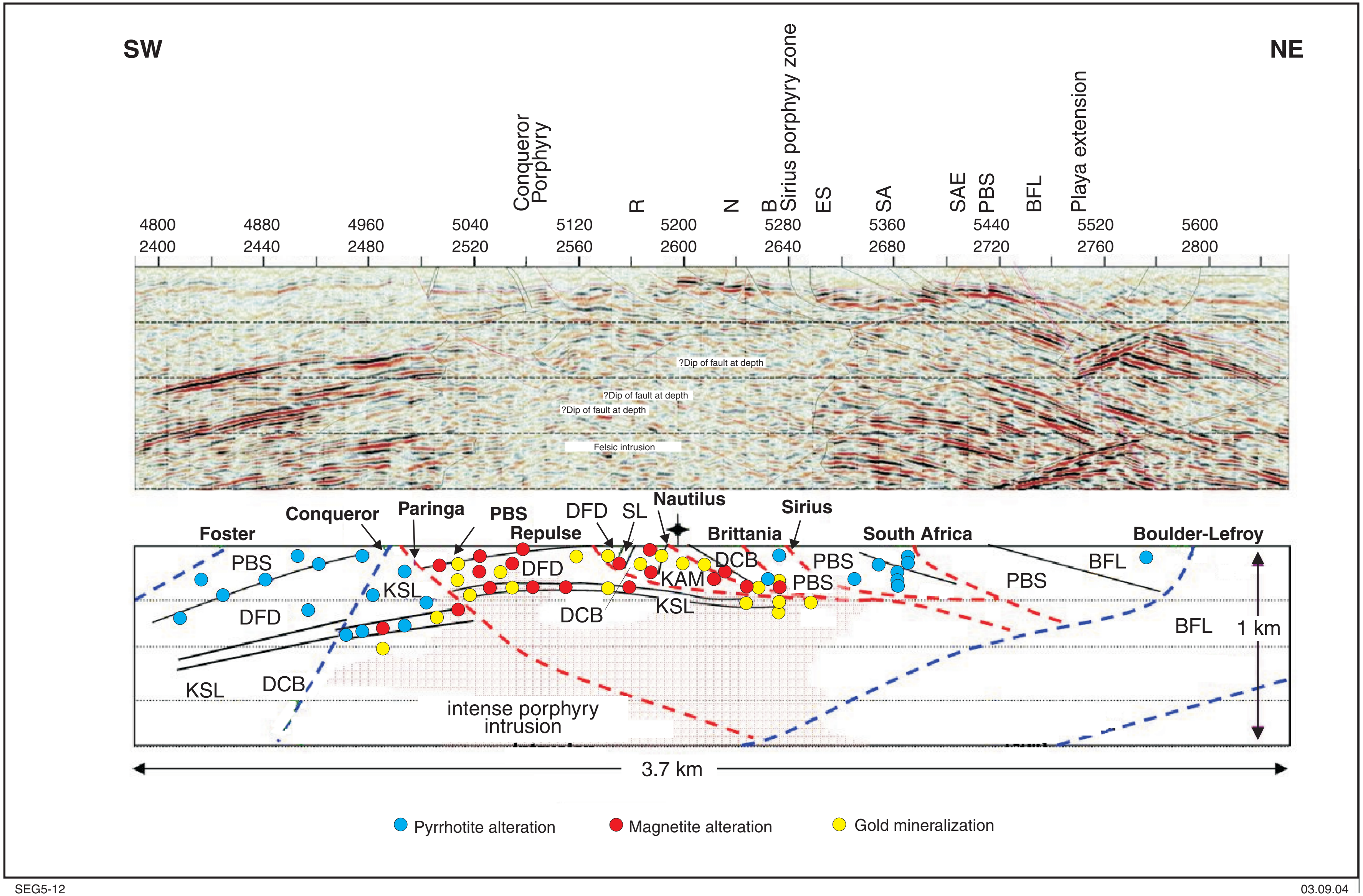

Figure 12. Cross section showing seismic data, and location of reduced and oxidized mineral assemblages, and gold mineralization. ES = East Sirius Thrust, R = Repulse Thrust, SA = South Africa Fault, SAE = South Africa East Fault. Other abbreviations as in Figures 5 and 8

This model requires that the two fluids migrate along different fluid conduits. Linking structures between these conduits provide zones where these fluids with grossly different redox conditions mixed. During the mixing process, the redox conditions of the hydrothermal fluid changed rapidly and resulted in gold precipitation, explaining the location of high-grade gold mineralization in the mixing zones. It is assumed that other gold precipitation mechanisms, such as phase separation in the hydrothermal fluid and fluid-wallrock interactions, took place but played a subordinate role in producing high grade oreshoots.

Excursion route

Introduction

It is difficult to plan the exact excursion route in advance in an active mine environment. However, it is likely that the excursion will visit the Argo mine and a mine in the Greater Revenge area, and these deposits are described below. The excursion will also inspect typical diamond drillcore showing hydrothermal alteration and ore mineral assemblages.

Argo gold deposit

Introduction

Argo is owned by the St Ives Gold Mining Company, a wholly owned subsidiary of Gold Fields. The Argo gold deposit was discovered in 1991 from aircore drilling targeting a distinct break in the airborne magnetic data over an interpreted dolerite unit. Follow-up drilling delineated a significant mineralized north-northeasterly trending structure referred to as the Argo Shear. Definition drilling commenced and an ore reserve was delineated by 1993. The deposit is currently being mined as both an openpit and underground operation. Past production and current reserves total 5 Mt at 5.8 g/t for about 930 000 ounces of gold, with a mineral resource of 7.2 Mt at 5.89 g/t for 1.38 Moz of gold as at July 2002. There is significant potential to increase the reserve and resource with increased exploration from underground.

Deposit geology and controls on mineralization

The Argo gold deposit is positioned on the western limb of the Kambalda – St Ives Antiform, to the west of the Boulder–Lefroy Fault, a major crustal-scale wrench fault system. The Condensor Dolerite, a 500 m-thick subvertical to southwesterly dipping differentiated sill, hosts the mineralization at Argo. The sill intruded along the contact between the Paringa Basalt and Black Flag Group.

The Argo deposit is a structurally complex, large mineralized shear system, which consists of the Argo Shear and a series of subsidiary mineralized shears. Gold mineralization at Argo is mainly confined to the Argo Shear, which strikes north and dips west, and extends over 800 m downdip. The shear system extends over a strike length of 1 km, and attenuates at the contact with the Paringa Basalt to the north, and the Black Flag Group to the south. Two easterly trending subvertical Proterozoic dolerite dykes crosscut the system. The Argo Shear is accompanied by a number of mineralized satellite structures. These include large, subparallel structures such as the H1 hangingwall shear, and lesser shallower dipping structures in the footwall positions (F2, and C1–3). The subhorizontal structures contain dilation vein sets, whereas steeper structures have a dominant (reverse fault) mylonitic component. The subparallel Apollo (A2 and A3) Shear bounds the eastern margin of the Argo system. The A2 Shear links with the Argo Shear at depth. Little is known about zones of mineralization beyond the H1 structure to the west, and the A2 and A3 structures to the east. The southern end of the deposit is covered by a sequence of Tertiary sediments, which are up to 60 m thick.

Three types of gold mineralization are evident at Argo:
- high-grade placer-style deposit hosted by quartz gravel at the base of the Tertiary cover sequence;
- supergene mineralization within the Tertiary sedimentary units and Archaean regolith;
- primary shear-hosted mineralization.

Greater Revenge deposits

Introduction

The Greater Revenge gold complex is almost entirely blind. The Revenge deposit itself was discovered beneath lake sediment cover in 1984 from diamond drilling to test magnetic anomalies in a favourable structural and stratigraphic setting. It was mined from 1989 to 1998. Subsequent discoveries have come from a lake exploration strategy using track-mounted aircore rigs for anomaly definition programs. However, credit must be given to 'old timers' (late 1890s) who were responsible for workings on Delta Island, which provide the only surface clue to mineralization in the area. Exploration of the Greater Revenge area, measuring 4.5 × 2.5 km, was started in 1994 and identified supergene gold anomalies. From 1997, progressive exploration delineated supergene pittable resources and significant primary ore. The >1 Moz potential of the system was recognized in 1998, but it was not until 2001 that the scale of the opportunity was appreciated, and programs were initiated to realise the full potential of the Greater Revenge area. From this time, accelerated exploration has added over 4 Moz to the inventory of modelled mineralization, above a cutoff of 0.8 g/t Au. The post-mined modelled inventory (total mineralization that has been captured in a model above a specified cutoff grade) above a 0.8 g/t cutoff has grown from 50 thousand ounces in 1998 to over 6.9 Moz in September 2003. About 3.7 million ounces of this was added between June 2002 and September 2003. The mineralized complex remains open to the north, south, and west, and at depth.

Deposit geology and controls on mineralization

The distribution of rocks in the area is controlled by the Delta Island Anticline, itself a segment of the Kambalda Anticline, which formed as a result of D_2 and subsequent minor D_3 folding events. The anticline is a gently plunging feature with a northwesterly striking D_2 major axis, and a northeasterly striking minor axis. The Tripod Hill Komatiite is situated within the core of the anticline, with conformably overlying and progressively younger Devon Consols Basalt, Kapai Slate, Defiance Dolerite, and Paringa Basalt. The numerous fractionated intermediate to felsic intrusions are dominantly concordant to subconcordant sills in the Greater Revenge area, and are folded with the stratigraphy, in contrast to more common steeply dipping dykes elsewhere in the field. The Tertiary lake sediments vary from being absent to 100 m thick. The dominant structural features in the Revenge area are the second order Playa, Belleisle, and Delta Shears. These structures strike north-northwest, but the Belleisle and Delta Shears dip westwards whereas the Playa Shear dips eastwards. Third-order reverse shears are shallow to steep, easterly or westerly dipping, and vary in strike from northwest to northeast. These third-order structures are the main hosts to mineralization, and include the Minotaur, Agamemnon, Mars, W66, N01, Delta, North Revenge, Kapai, West Revenge, and W series structures.

References

ARCHIBALD, N. J., 1979, Tectonic–metamorphic evolution of an Archaean terrain: a study of the Norseman–Widgiemooltha granitoid–greenstone belt, Eastern Goldfields Province, Western Australia: The University of Western Australia, PhD thesis (unpublished).

ARCHIBALD, N. J., 1985, The stratigraphy and tectono-metamorphic history of the Kambalda–Tramway area, Western Australia: Western Mining Corporation (unpublished).

BADER, K., 1994, Geology of the Merougil Formation, Kambalda, Western Australia: Monash University, BSc Honours thesis (unpublished).

BALKAU, J., 1989, Exploration history, Junction gold orebody: Western Mining Corporation (unpublished).

BARLEY, M. E., BROWN, S. J., KRAPEZ, B., and CAS, R. A. F., 2002, Tectono-stratigraphic analysis of the Eastern Yilgarn Craton: an improved framework for exploration in Archaean terrains: Australian Mineral Industry Research Institute, Final Report for AMIRA P437, 200p.

BATEMAN, R., 2001, Archaean gabbros and basalts (Kalgoorlie); geochemistry and tectonics in time, *in* Fourth International Archaean Symposium extended abstracts *edited by* K. F. CASSIDY, J. M. DUNPHY, and M. J. VAN KRANENDONK: AGSO – Geoscience Australia, Record, no. 2001/37, p. 124–126.

BAVINTON, O. A., 1979, Interflow sedimentary rocks from the Kambalda ultramafic sequence: their geochemistry, metamorphism and genesis: The Australian National University, PhD thesis (unpublished).

BENNET, M. A., 1995, The structure and timing of gold mineralization in the Victory area and its relationship to regional deformation in the eastern Goldfields: Western Mining Corporation (unpublished).

BLEWETT, R. S., CASSIDY, K. F., CHAMPION, D. C., and WHITAKER, A. J., 2004, The characterisation of granite deformation events in time across the Eastern Goldfields Province, Western Australia: Geoscience Australia, Record, no. 2004/10 (CD-ROM).

BLEWETT, R. S., CASSIDY, K. F., CHAMPION, D. C., HENSON, P. A., GOLEBY, B. S., JONES, L., and GROENEWALD, P. B., in press, The Wangkathaa Orogeny: an example of episodic regional 'D_2' in the late Archaean Eastern Goldfields Province, Western Australia: Precambrian Research.

CAREY, M. C., 1994, Petrography and geochemistry of selected sills from the Kambalda–Kalgoorlie region, W.A.: The Australian National University, BSc Honours thesis (unpublished).

CHAUVEL, C., DUPRE, B., and JENNER, G. A., 1985, The Sm–Nd age of Kambalda volcanics is 500 Ma too old!: Earth and Planetary Science Letters, v. 74, 315-324.

CLAOUÉ-LONG, J. C., COMPSTON, W., and COWDEN, A. C., 1988, The age of the Kambalda greenstones resolved by ion-microprobe: implications for Archaean dating methods: Earth and Planetary Science Letters, v. 89, p. 239–259.

CLARK, M. E., 1987, The geology of the Victory gold mine, Kambalda, Western Australia: Queens University, PhD thesis (unpublished).

CLARK, M. E., ARCHIBALD, N. J., and HODGSON, C. J., 1986, The structural and metamorphic setting of the Victory gold mine, Kambalda, Western Australia, *in* Proceedings of Gold '86 *edited by* A. J. Macdonald: Toronto, Canada, Konsult International, p. 243–254.

CLARK, M. E., CARMICHAEL, D. M., HODGSON, C. J., and FU, M., 1989, Wall-rock alteration, Victory Gold Mine, Kambalda, Western Australia: processes and P–T–X(CO_2) conditions of metasomatism, *in* The geology of gold deposits: the perspective in 1988 *edited by* R. R. KEAYS, W. R. H. RAMSAY, and D. I. GROVES: Economic Geology Monograph 6, p. 445–456.

CLOUT, J. M. F., 1991, Geochronology of the Kambalda–Kalgoorlie area: a review: Western Mining Corporation (unpublished).

COMPSTON, W., WILLIAMS, I. S., CAMPBELL, I. H., and GRESHAM, J. J., 1986, Zircon xenocrysts from the Kambalda volcanics: age constraints and direct evidence for older continental crust below the Kambalda–Norseman greenstones: Earth and Planetary Science Letters, v. 76, p. 299–311.

CONNORS, K., DONALDSON, J., MORRISON, R., and DAVY, C., 2003, Internal technical note TN SIG0329: the stratigraphy of the Kambalda – St. Ives district. Gold Fields Ltd (unpublished).

COWDEN, A. C., and ARCHIBALD, N. J., 1987, Kambalda–Kalgoorlie stratigraphy: evidence of volcanic cycles and structural repetition in Archaean greenstones: Western Mining Corporation (unpublished).

COWDEN, A. C., and ROBERTS, D. E., 1990, Komatiite hosted nickel sulphide deposits, Kambalda, *in* Geology of the mineral deposits of Australia and Papua New Guinea *edited by* F. E. HUGHES: The Australasian Institute of Mining and Metallurgy, Monograph 14, v. 1, p. 567–581.

COX, S. F., and RUMING, K., 2004, The St Ives mesothermal gold system, Western Australia — a case of golden aftershocks?: Journal of Structural Geology, v. 26, p. 1109–1125.

DONALDSON, M. J., 1983, Progressive alteration of barren and weakly mineralised Archean dunites: a petrological, mineralogical and geochemical study of some intrusive dunites from Western Australia: The University of Western Australia, PhD thesis (unpublished).

FOSTER, J. G., 1993, Applications of rare earth element (REE) and Re–Os isotope geochemistry to the exploration for komatiite hosted nickel sulphide deposits: Western Mining Corporation (unpublished).

GEE, R. D., 1979, Structure and tectonic style of the Western Australian Shield: Tectonophysics, v. 58, p. 327–369.

GEE, R. D., BAXTER, J. L., WILDE, S. A., and WILLIAM, I. R., 1981, Crustal development in the Archaean Yilgarn Block, Western Australia, *in* Archaean geology, Second International Symposium, Perth, 1980 *edited by* J. E. GLOVER and D. I. GROVES: Geological Society of Australia, Special Publication, no. 7, p. 43–56.

GOLEBY, B. R., RATTENBURY, M. S., SWAGER, C. P., DRUMMOND, B. J., WILLIAMS, P. R., SHERATON, J. W., and HEINRICH, C. A., 1993, Archaean crustal structure from seismic reflection profiling, Eastern Goldfields, Western Australia: Australian Geological Survey Organisation, Record, no. 1993/15, p. 54.

GOODGAME, V. R., 1997, The distribution and origin of arsenic and platinum group element mineralisation in the Mariners nickel deposit, Widgiemooltha, Western Australia: University of Oregon, PhD thesis (unpublished).

GRESHAM, J. J., and LOFTUS-HILL, G. D., 1981, The geology of the Kambalda nickel field, Western Australia: Economic Geology, v. 76, p. 1373–1416.

HAND, J., 1996, Mineralised volcanic and sedimentary environments in the Eastern Goldfields: Western Mining Corporation (unpublished).

HAYWARD, N. L., 1988, Geology of the Widgiemooltha area and exploration progress to February 1988: Western Mining Corporation (unpublished).

HILL, R. I., CHAPPELL, B. W., and CAMPBELL, I. H., 1992, Late Archaean granites of the southeastern Yilgarn Block, Western Australia: age, geochemistry and origin: Transactions of the Royal Society of Edinburgh, Earth Sciences, v. 83, p. 211–226.

KRAPEZ, B., BROWN, S. J. A., HAND, J., BARLEY, M. E., and CAS, R. A. F., 2000, Age constraints on recycled crustal and supracrustal sources of Archaean metasedimentary sequences, Eastern Goldfields Province, Western Australia: evidence from SHRIMP zircon dating: Tectonophysics, v. 322, p. 89–133.

LESHER, C. M., and ARNDT, N. T., 1995, REE and Nd isotope geochemistry, petrogenesis, and volcanic evolution of contaminated komatiites at Kambalda, Western Australia: Lithos, v. 34, p. 127–157.

MacGEEHAN, P. J., 1984, Internal zonation: Victory Dolerite: Western Mining Corporation (unpublished).

MARSH, S., 1988, Origin of the magnetite-rich facies Kapai Slate, Kambalda, Western Australia: The University of Western Australia, PhD Honours thesis (unpublished).

McCALL, G. J. H., 1969, The Archaean succession to the west of Lake Lefroy: Journal of the Royal Society of Western Australia, v. 52, p. 119–128.

McNAUGHTON, N. J., and DAHL, N., 1987, A geochronological framework for gold mineralisation in the Yilgarn Block, Western Australia, *in* Recent advances in understanding Precambrian gold deposits *edited by* S. E. HO and D. I. GROVES: Geology Department and University Extension, The University of Western Australia, Publication, no. 11, p. 29–49.

NEALL, F. B., and PHILLIPS, G. N., 1988, Fluid-wall rock interaction in an Archean hydrothermal gold deposit: a thermodynamic model for the Hunt mine, Kambalda: Economic Geology, v. 82, p. 1679–1694.

NEUMAYR, P., HAGEMANN, S. G., WALSHE, J., and MORRISON, R. S., 2003, Camp- to deposit-scale zonation of hydrothermal alteration in the St Ives gold camp, Yilgarn Craton, Western Australia: evidence for two fluid systems?, *in* Mineral exploration and sustainable development, Seventh Biennial SGA Meeting, Athens, 2003, abstracts: Athens, Greece, Society for Geology Applied to Mineral Deposits, p. 799–802.

NGUYEN, T. P., 1997, Structural controls on gold mineralization at the Revenge Mine and its tectonic setting in the Lake Lefroy area, Kambalda, Western Australia: The University of Western Australia, PhD thesis (unpublished).

NGUYEN, T. P., COX, S. F., HARRIS, L. B., and POWELL, C. M., 1998, Fault-valve behaviour in optimally oriented shear zones: an example at the Revenge gold mine, Kambalda, Western Australia: Journal of Structural Geology, v. 20, p. 1625–1640.

NGUYEN, T. P., GOODWIN, D., WILKINSON, C., and WITHERS, J., 1992, Kambalda gold targeting criteria: Western Mining Corporation (unpublished).

PERRIAM, R. P. A., 1985, The tectonic evolution of the Mt Martin – Carnilya Hill district of the Eastern Goldfields, Western Australia: The University of Western Australia, MSc thesis (unpublished).

POLITO, P. A., BONE, Y., CLARKE, J. D. A., and MERNAGH, T. P., 2001, Compositional zoning of fluid inclusions in the Archaean Junction gold deposit, Western Australia: a process of fluid–wall-rock interaction?: Australian Journal of Earth Sciences, v. 48, p. 833–855.

REDMAN, B., and KEAYS, R. R., 1985, Archaean basic volcanism in the Eastern Goldfields Province, Yilgarn Block, Western Australia: Precambrian Research, v. 30, p. 113–152.

ROBERTS, D. E., and ELIAS, M., 1990, Gold deposits in the Kambalda–St Ives region, *in* Geology of the mineral deposits of Australia and Papua New Guinea *edited by* F. E. HUGHES: The Australasian Institute of Mining and Metallurgy, Monograph 14, v. 1, p. 479–491.

ROCK, N. M., TAYLOR, W. R., and PERRING, C. S., 1990, Lamprophyres, *in* Gold deposits of the Archaean Yilgarn Block, Western Australia: nature, genesis and exploration guides *edited by* S. E. HO, D. I. GROVES, and J. M. BENNETT: Geology Department (Key Centre) and University Extension, The University of Western Australia, Publication, no. 20, p. 128–135.

SWAGER, C. P., and GRIFFIN, T. J., 1990, An early thrust duplex in the Kalgoorlie–Kambalda greenstone belt, Eastern Goldfields Province, Western Australia: Precambrian Research, v. 48, p. 63–73.

WATCHORN, R. B., 1998, Kambalda – St Ives gold deposits, *in* Geology of Australian and Papua New Guinean mineral deposits *edited by* D. A. BERKMAN and D. H. MacKENZIE: The Australasian Institute of Mining and Metallurgy, Monograph 22, p. 243–254.

WILLIAMS, P. R., and WHITAKER, A., 1993, Gneiss domes and extensional deformation in the Archaean Eastern Goldfields Province, Western Australia: Ore Geology Reviews, v. 8, p. 141–162.

WONG, T., 1986, Metamorphic patterns in the Kambalda area and their significance to Archaean greenstone belts of the Kambalda–Widgiemooltha area: The University of Western Australia, BSc (Honours) thesis (unpublished).

WOODALL, R., 1990, Gold in Australia, *in* Geology of the mineral deposits of Australia and Papua New Guinea *edited by* F. E. HUGHES: The Australasian Institute of Mining and Metallurgy, Monograph 14, v. 1, p. 45–67.